INFORMATION TO USERS

This manuscript has been reproduced from the microfilm master. UMI films the text directly from the original or copy submitted. Thus, some thesis and dissertation copies are in typewriter face, while others may be from any type of computer printer.

The quality of this reproduction is dependent upon the quality of the copy submitted. Broken or indistinct print, colored or poor quality illustrations and photographs, print bleedthrough, substandard margins, and improper alignment can adversely affect reproduction.

In the unlikely event that the author did not send UMI a complete manuscript and there are missing pages, these will be noted. Also, if unauthorized copyright material had to be removed, a note will indicate the deletion.

Oversize materials (e.g., maps, drawings, charts) are reproduced by sectioning the original, beginning at the upper left-hand corner and continuing from left to right in equal sections with small overlaps.

ProQuest Information and Learning
300 North Zeeb Road, Ann Arbor, MI 48106-1346 USA
800-521-0600

Université d'Ottawa • University of Ottawa

Abstract

The effect of the support in heterogeneous catalysis is very important but often poorly understood. The reaction of tetraneopentylchromium(IV) with Sylopol 952, a silica gel used industrially as a carrier for α-olefin polymerization catalysts, has been investigated and compared with the previously reported reaction on Aerosil 200, a fumed silica often used to model catalyst supports. Grafting, thermolysis, and metathetical exchange reactions of chromium(IV) neopentylidenes were found to be the same on either Aerosil 200 or Sylopol 952. However, reactivity of the grafted organochromium fragments towards ethylene was found to be quite different on the two supports.

The research described in this thesis also explores the polymerization activity of bis(neopentyl)chromium(IV) fragments at higher ethylene pressures than were previously investigated. This result has greatly altered thinking about the nature of the active site for olefin polymerization over surface organochromium fragments. The supported bis(neopentyl)chromium(IV) is no longer believed to require thermal activation to create chromium alkylidene active sites. A possible mechanism is postulated.

Propylene polymerization by the Aerosil-supported chromium alkylidene was observed as a slow pseudo-first-order reaction. The kinetics were examined at the gas-solid interface by *in situ* FTIR spectroscopy and the second-order rate constant compared to those previously measured for ethylene and 1-hexene.

Acknowledgements

First and foremost, I am most indebted to Dr. Susannah L. Scott, my dear research supervisor, not only for giving me the opportunity to work on this project but also for her infinite patience, encouragement, being a very understanding person and lots more I gained from her. She is always there to help and encourage no matter when and what. Without her, I would still be lost to this day. For every chance I was given to stumble and fail as I tried to find my way, I was given so many chances to find the answers and succeed. She is such a blessed capable person that being able to make others more complete. Again, thank you so much, Susannah, for giving me the time and the environment to develop as a true scientific professional and a person even though I am still far away from a good chemist.

Secondly, I would like to thank Dr. Marten Ternan for offering such an interesting lecture and being a very kind person. He too is blessed with infinite patience. His generous amount of time giving me and technical advice make me smarter to make decisions and better understand being a professional.

And, speaking of lab environment, I am sure that I owe most of the knowledge that I have acquired over the past several years to my labmates, Tamara L. Church, Marcel C. Beaudoin, Ziyad M. Taha, Omisola Womiloju, Dao Nguyen, Lenny MacAdams, Valbona Celo, Nazafarin Lahoutifard, Ludmila Nossova and all the other undergraduates, graduate students, and postdocs.

I would also thank the entire Chemistry Department support staff for their technical support and for their time.

I would give my sincere acknowledgements to my family whom I love very much. You are always there to support me whenever I feel weak and down. This thesis is every bit as much as yours as it is mine.

Finally, I would like to thank my best friend Yi, for her support and encouragement particularly during the period of writing up this thesis.

Table of Contents

Chapter 2. Experimental Techniques

List of Figures

Chapter 1

Chapter 2

Chapter 3

Chapter 4

List of Schemes

Chapter 1

Chapter 3

Chapter 4

List of Tables

Chapter 1

.

Chapter 3

Chapter 4

Chapter 1

Introduction

1.1 Catalytic olefin polymerization

Polyolefins are polymers based on saturated hydrocarbons with only single C-C bonds. They are the most widely used polymers in the world. Of the polyolefins, by far the largest-volume plastic is polyethylene. It was originally discovered in ICI in 1933. The first synthesis involved free radical polymerization of ethylene under severe reaction conditions (2000 bar, 200°C).[1] This process has been largely supplanted by the catalytic polymerization of ethylene, which has the significant advantage of operating at substantially lower temperatures and pressures.

One of the main industrial uses for catalysts is the polymerization of olefins. The chain growth reactions involved in olefin oligomerization and polymerization are governed by a sequence of initiation, propagation, and termination steps. Propagation and termination are depicted in equation 1.1:

$$\begin{array}{ccccccc} & & k_1 & & k_1 & & k_1 \\ \ldots \rightarrow & M(R)_{n-1} & \rightarrow & M(R)_n & \rightarrow & M(R)_{n+1} & \rightarrow \ldots \\ & & \downarrow k_2 & & \downarrow k_2 & & \downarrow k_2 \\ & & R_{n-1} & & R_n & & R_{n+1} \end{array} \qquad (1.1)$$

where M = metal and R = monomer. The distribution of chain lengths for the growth reaction can be represented mathematically as the Schulz-Flory distribution, according to equation 1.2.

$$W_n = n\alpha^{n-1}(1-\alpha)^2, \quad \text{where } \alpha = k_1/(k_1+k_2) \qquad (1.2)$$

W_n represents the weight fraction, and k_1, k_2 are the rate constants for the propagation and termination steps respectively. A plot $\ln(W_n/n)$ vs. C_n (number of carbons) is linear, with a slope of $\ln\alpha$. Thus the k_1/k_2 ratio can be obtained.

Three extreme situations are possible:

a) $k_1 >> k_2$ propagation dominates over termination and high molecular weight polymer is the result.

b) $k_1 << k_2$ termination is much more rapid than propagation and selective dimerization can be achieved.

c) $k_1 \approx k_2$ representative of the more typical intermediate situation, the rate constants are of comparable value, and the Schulz-Flory distribution of C_n products is obtained.

The advantages of catalytic polymerization are not limited to operation at low temperatures and pressures. The presence of a catalyst also offers the ability to modify polymer microstructure. The1963 Nobel Prize for Chemistry was awarded to Professors Ziegler and Natta for their pioneering discoveries of catalysts for olefin polymerization.

1.1.1 Commercial classification of polyethylene

Polyethylene is by far the most widely used commodity polymer in the world. Global polyethylene production now exceeds 40 million tons annually.[2] There are three commercially important varieties: (1) high density polyethylene (HDPE); (2) low density polyethylene (LDPE); (3) linear low density polyethylene (LLDPE). HDPE is the most important; it is a linear polymer with m.p. of about 136°C. It can be made by three different commercial processes: solution, slurry and gas phase. They are all performed at ethylene pressures of less than 50 atm. LDPE is prepared at high pressures and temperatures with free radical initiators. Finally, LLDPE is usually manufactured by the metal-catalyzed copolymerization of ethylene with α-olefins.

1.1.2 Homogeneous vs heterogeneous catalysts

Despite the availability of finely-tuned homogeneous catalysts for olefin polymerization, heterogeneous systems are overwhelmingly the catalysts of choice in

industrial practice. Many of the reasons are related to reactor design and process control. Heterogeneous catalysts are capable of operating in the absence of solvent (gas phase polymerization) resulting in considerable capital savings. Heterogeneous catalysts are also less susceptible to the production of polymer fines and reactor fouling, since polymer morphology replicates that of the macroscopic catalyst particles. Heterogeneous catalysts tend to deactivate more slowly than their homogeneous counterparts, resulting in greater catalyst productivity. Finally, heterogeneous catalysts generate polyolefins with broad molecular weight distributions, which facilitate processing.

Heterogeneous catalytic systems in olefin polymerization have at least two components: a transition metal catalyst and a catalyst support. Many also require a Lewis acid activator (i.e., co-catalyst). In the following sections, transition metal catalysts and catalyst supports will be discussed.

1.2 Metal catalysts for coordination polymerization of α-olefins

The most widely-used transition metal catalysts for heterogeneous polymerization of olefins are summarized in **Table 1.1**.

Table 1.1 Polyolefins produced with transition metal catalysts

Polymer	Major catalysts
High-density polyethylene	$TiCl_x/AlR_3$, Cr/silica
Linear low-density polyethylene	$TiCl_x/AlR_3$, Cr/silica
Polypropylene	$TiCl_x/AlR_2Cl$, $TiCl_4MgCl_2$
Ethylene/propylene/diene elastomers	$VOCl_3/AlR_2Cl$, $TiCl_4/MgCl_2/AlR_2Cl$, $ZrCp_2Cl_2$/MAO[a]
Cis-1,4-polybutadiene	TiI_4/AlR_3, $Co(O_2CR)_2/Al_2R_3Cl_3$, $Ni(O_2CR)_2/AlR_3/BF_3$

[a] MAO = methylaluminoxane, Cp = cyclopentadiene.

1.2.1 Mechanism of metal-catalyzed olefin polymerization

Four propagation mechanisms have been proposed for metal-catalyzed olefin polymerization: the Cossee,[3] Green-Rooney,[4] Green-Rooney-Brookhart[5,6,7] and the hybrid Cossee/Green-Rooney-Brookhart mechanisms.

The Cossee mechanism requires a vacant site on the metal center for olefin monomer to coordinate to the metal at this site. Migratory insertion extends the growing alkyl chain by one monomer unit, **Scheme 1.1**. This mechanism is by far the most commonly accepted.

Scheme 1.1 Cossee mechanism

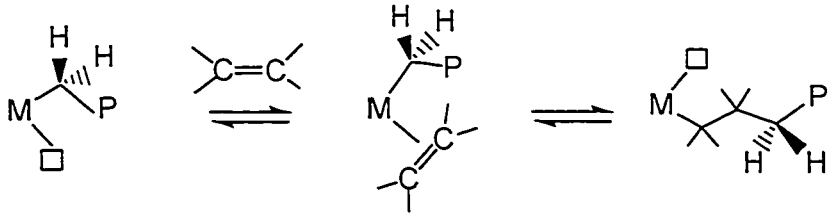

The Green-Rooney mechanism requires two vacant coordination sites at the metal center. An α-hydride elimination from the growing polymer chain to the metal generates a transient carbene. Olefin coordination and [2+2] cycloaddition give a metallacycle. Reductive elimination cleaves the ring and produces an alkyl chain extended by one monomer unit, **Scheme 1.2**.

Scheme 1.2 Green-Rooney mechanism

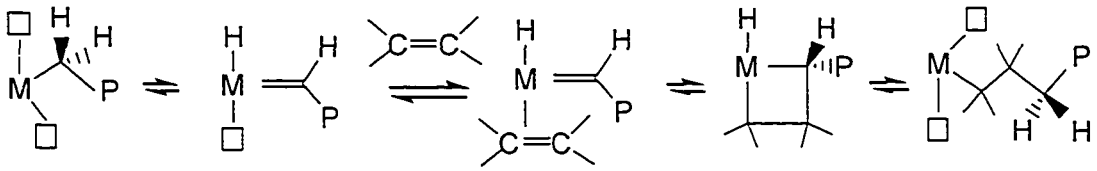

The Green-Rooney-Brookhart mechanism is intermediate between two previous mechanisms. The α-hydrogen is not completely transferred to the metal but interacts with the metal through a three-membered, two-electron "agostic interaction".[8] In the fourth and last mechanism, the hybrid Cossee/Green-Rooney-Brookhart, the α-agostic interaction occurs only during the transition state.

1.2.2 Ziegler-Natta catalysts

Classical Ziegler-Natta catalysts are heterogeneous materials formed by interaction of $TiCl_3$ and Al alkyls, or $TiCl_4$ supported on $MgCl_2$, with $AlEt_3$ as co-catalyst. They are active at 25°C and 1 bar, in sharp contrast to the severe conditions required for the original thermal, radical-initiated polymerization of ethylene. Approximately 60% of worldwide production capacity of polyolefins is manufactured using these two-component catalysts. They are complex systems with several active sites. Non-uniformity of the active sites renders mechanistic study and rational design of modified catalysts extremely difficult. However, the reaction mechanism of Ziegler-Natta

catalysts is largely agreed to follow the Cossee pattern (**Scheme 1.1**) based on extensive studies of well-defined molecular (metallocene) analogues.

1.2.3 Supported chromium catalysts

Alternatives to Ziegler-Natta catalysts, especially for the manufacture of polyethylene, are the one-component chromium-based catalysts. About one-third of HDPE is manufactured using chromium catalysts,[9] in which Cr is bound to a high-surface area support such as silica. Phillips catalysts are based on inorganic chromium, distinguishing them from organometallic chromium catalysts, such as the Union Carbide catalyst.

1.2.3.1 Phillips catalysts

The Phillips catalytic system consists of an inorganic Cr compound such as CrO_3 and an oxide support, typically silica. Phillips catalysts are both cheaper and more robust than Ziegler-Natta catalysts and, unlike the Ziegler-Natta catalysts, do not require a co-catalyst. Since its discovery in the early 1950's, the Phillips system has inspired great interest in fundamental research due to its ability to initiate polymerization without an exogeneous source of alkyl ligands.

A typical Phillips catalyst is prepared by impregnating silica with a chromium salt or oxide.[10,11] Upon dehydroxylation of the silica surface by calcination, chromium is anchored and oxidized to Cr(VI), equation 1.3.

$$2 \equiv SiOH + CrO_3 \rightarrow (\equiv SiO)_2CrO_2 + H_2O \qquad (1.3)$$

An induction period is usually observed prior to initiation of polymerization. During this time, chromium is reduced from its highest oxidation state (VI) to lower ones. The main chromium oxidation state after reduction is divalent, equation 1.4.[12]

$$(\equiv SiO)_2CrO_2 + C_2H_4 \rightarrow (\equiv SiO)_2Cr + 2\ CH_2O \qquad (1.4)$$

Although the Cr(II) form of the catalyst is active for ethylene polymerization without an induction period, (II) is unlikely to be the oxidation state of Cr during propagation of the polymer chain.[13,14] Mechanisms for initiation require Cr-H or Cr-C bond formation and hence involve higher oxidation states of Cr. Proposals include oxidative addition of a surface hydroxyl group, of ethylene, or rearrangement of coordinated ethylene to an alkylidene or metallacyclic species,[15,16] **Figure 1.1**.

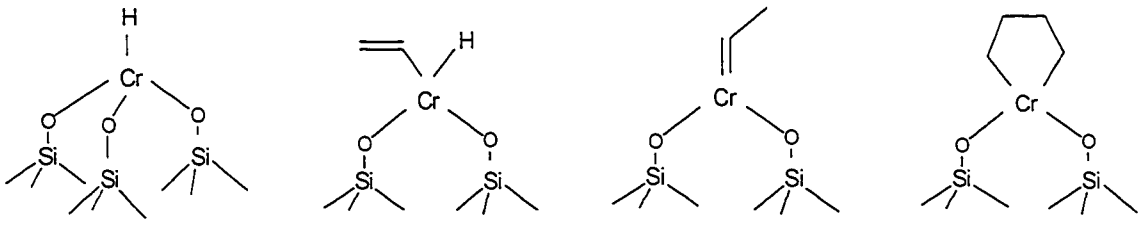

Figure 1.1 Some proposed initiating sites on Phillips catalysts.

In these structures, Cr(IV) is present and may be the active site for propagation.[17,18] However, experimental studies have failed to produce convincing evidence to support the presence of any of these species on the catalyst surface. The observation of a vibration at 2750 cm^{-1} was originally assigned to alkylidene active sites,[19] but was later questioned.[20] The extremely low number of propagation sites on various Phillips-type catalysts, with estimates ranging from 0.01 to 10%,[21,22] renders the initiating sites virtually invisible to spectroscopic probes and makes it very difficult to investigate the propagation mechanism in Phillips systems.

1.2.3.2 Organochromium catalysts

Chromocene, Cp_2Cr, grafted onto highly dehydroxylated silica produces another type of ethylene polymerization catalyst. These organochromium catalysts were first discovered in the early 1970's and developed by F. Karol et al. at Union Carbide.[23] Although Cr is initially present in the (II) oxidation state, and the catalyst shows no

induction period, the grafted species has no Cr-C bond for olefin insertion. Thus initiation and propagation on Carbide catalysts are also mechanistically mysterious.

1.3 Surface organometallic models for Phillips catalysts

Surface organometallic chemistry (SOMC)[24,25] is the study of the reactivity of well-defined organometallic compounds with surfaces. SOMC attempts to define the nature of the interaction of the surface layer with organometallic molecules by limiting the interaction to a monolayer during reactions. The surfaces of many inorganic oxides, such as silicas, zeolites, etc., can be treated as ligands towards the organometallic reagent.

Surface organometallic models are required where molecular model compounds are inadequate. For example, Carrier et al. attempted to model the Phillips catalyst by employing bis(triphenylsilyl)chromate in cyclohexane,[26] **Scheme 1.3**.

Scheme 1.3 Homogeneous model of Phillips catalyst

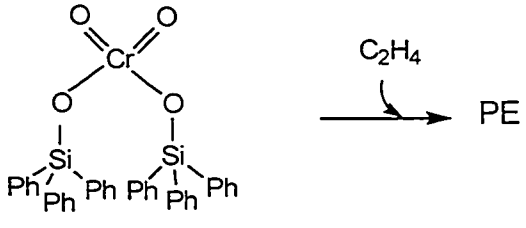

At low ethylene pressures (< 300 psi), this solution gives little or no high molecular weight polyethylene. However, when the molecular chromium complex is deposited onto high surface area silica-alumina, a very active catalyst is obtained.

Therefore, models based on the assumption that the silica support is inert during polymerization are inadequate. The nature of the silica is known to be particularly important in determining the activity of supported polymerization catalysts.[27] Surface organometallic model catalysts are actively being sought. The model must incorporate a well-defined molecular chromium compound and the silica acting as a ligand towards chromium.[28]

1.4 Silica supports

1.4.1 Surface chemistry

Silicas are widely used in chemical analysis and preparations, as adsorbates and fillers,[29,30] acid catalysts[31,32] and as catalyst supports,[33,34] due to their thermal stability, chemical durability, high purity and thermal shock resistance.[35] The usefulness of silica has stimulated much research for better understanding of its morphology, porosity and surface characteristics.[36] The surface of silica is composed of unreactive siloxanes, ≡SiOSi≡, and a variety of silanols. It has long been recognized that the key to the adsorption behavior of molecular compounds on silica surfaces is

the silanol.[37,38,39,40,41,42,43] Unsaturated surface valencies are balanced by these surface hydroxyl functionalities, whose distribution is temperature-dependent. During the past thirty years, a great deal of theoretical and experimental studies have been conducted on silanols, including their (1) classification; (2) spectroscopic characterization; (3) effect of thermal treatment; (4) effect of silanol type and population on acidity of silica; (5) effect of silica microstructure on reactivity. Four types of silanol groups have been identified on silica surfaces: (a) isolated (free); (b) vicinal; (c) geminal; (d) hydrogen-bonded, **Figure 1.2**.

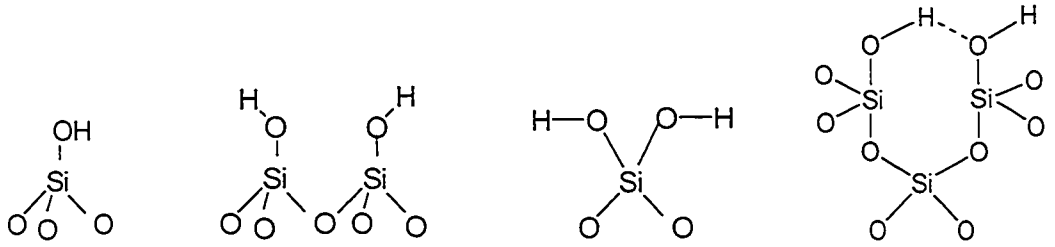

Figure 1.2 Schematic presentation of four types of silanol groups present on silica surfaces: (a) isolated (free); (b) vicinal (non-hydrogen bonded); (c) geminal; (d) hydrogen-bonded.

The molecular surface properties of silicas have been investigated using vibrational spectroscopies, particularly FTIR. When silicas are subjected to a high

temperature for a certain period of time, adjacent silanol groups condense to form a siloxane bridge by eliminating H_2O, equation 1.5.

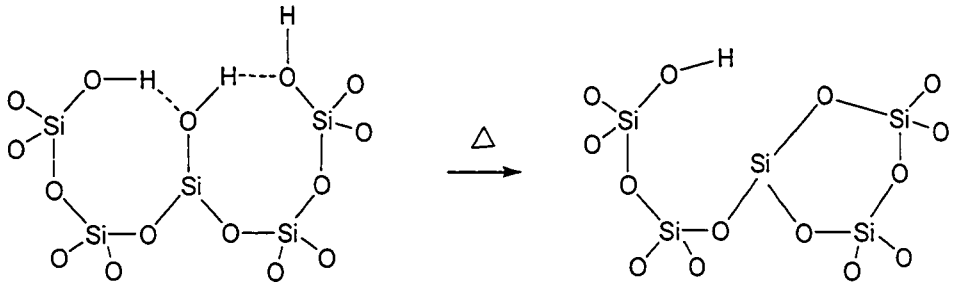

(1.5)

IR spectroscopy provides evidence for the changes that occur on silica surfaces during various thermal treatments. The peak at 3747 cm^{-1} due to isolated silanols increases in intensity and becomes more symmetrical, whereas the broad shoulder at ca. 3690 cm^{-1} due to hydrogen-bonded hydroxyl groups decreases in intensity. **Figure 1.3** clearly shows this trend on two types of silica (Aerosil 200 and Sylopol 952) as the temperature increases. At the same time, the quantity of surface siloxanes increases with the dehydration temperature.

The work of Ong et al. demonstrated that silanols can be classified into two groups by their respective pK_a values.[44,45] Silanols with pK_a = 4.9 are believed to be isolated and on a fully hydrated surface comprise only 19% of the silanol population, whereas the remainder (81%), with pK_a = 8.5, are hydrogen-bonded silanols. Regardless of the type of silica used, the protons of the surface hydroxyl groups underwent ion-exchange readily with metal cations, a key step in catalyst preparation that is related to the Brønsted acidity of the silanol groups.

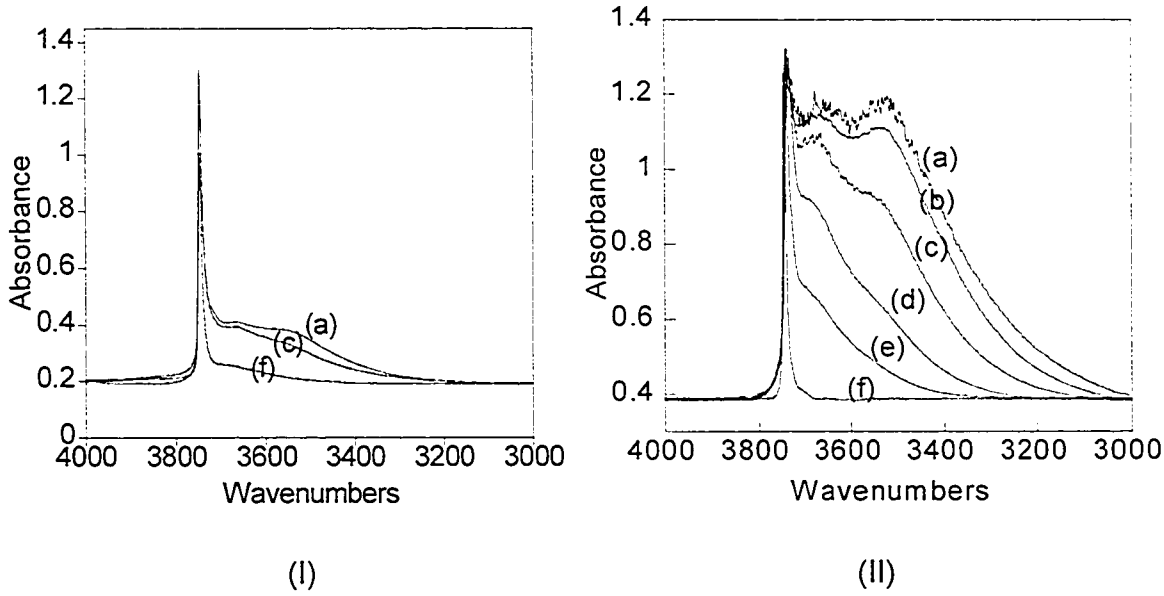

Figure 1.3 IR spectra of (I) Aerosil 200 silica and (II) Sylopol 952 silica after treatment at (a) 25°C; (b) 100°C; (c)200°C; (d) 300°C; (e) 400°C; (f) 500°C.

Peri et al. represent the surface of amorphous silica using the (100) face of β-cristobalite.[46] **Figure 1.4** shows this surface, in which the Si-O-Si bond angles are 180°. When the surface is fully hydrated, each surface silicon atom is bound to two hydroxyls. The surface then holds 7.9 hydroxyl groups per 100 Å, and H-bonding presumably occurs between silanols on adjacent silicon atoms. Silanols condense to form H_2O when hydroxyl groups on adjacent silicon atoms form a siloxane link. Condensation of two hydroxyls on the same silicon atom (geminal pair) is unlikely since silicon does not form >Si=O groups readily.

1.4.2 Silica types

There are three forms of silica other than minerals: fumed, precipitated and silica gels. Gel silicas are highly porous, fumed silicas are not, and precipitated silicas are in between. Aerosil 200 and Sylopol 952 silicas were used in this research in order to better understand the influence of the support on Cr catalyst behavior. The preparation, general physical properties, surface structure, IR characterization, and reactivity of these two types of silicas are described and compared in the following sections.

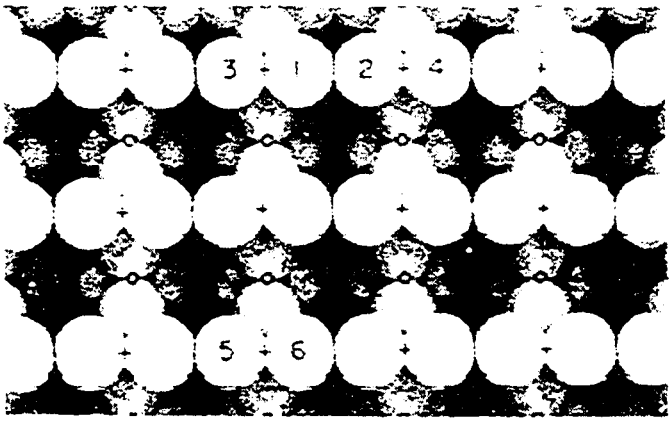

Figure 1.4 The β-cristobalite (100) face. Geminal silanols (white) are held by silicon atoms in interstices beneath the + signs. Other silicon atoms are held in interstices beneath the small circles.[48]

1.4.2.1 Aerosil 200

Aerosils are a family of fumed silicas from Degussa AG (Frankfur, FRG).[47] They are produced by reaction of $SiCl_4$ with O_2 in a flame. The result is small, non-porous particles of high purity (> 99.8%) silicon dioxide, which is also called pyrogenic silica. The surface area is determined by the residence time of particles in the flame. Aerosil 200 is a fumed silica with a specific surface area in the range 175-225 m^2/g. The primary particles of this amorphous silica have an average size of 12 nm (by TEM). The local surface geometry of Aerosil 200 is nearly planar, characterized by a fractal exponent for D_s close to 2.[48] The pH value of a 4% slurry of this silica is in the range 3.7-4.7.[49]

IR spectra of Aerosil 200 silica after different thermal treatments are shown in **Figure 1.3**. The spectra show the presence of isolated silanols at 3747 cm^{-1} and hydrogen-bonded silanols between 3700-3200 cm^{-1}. The silanol groups confer hydrophilic character upon the Aerosil. However, as they are eliminated by thermal treatment, the silica becomes progressively more hydrophobic. The number of accessible silanol groups after different thermal treatments, as determined by $VOCl_3$ chemisorption, is shown in **Table 1.2**.

Because of their production cost, Aerosils are not cost-effective as catalyst supports, although they have found widespread use in studies of catalysts because of their ready availability, high and reproducible purity, and ease of use in spectroscopic

Table 1.2 Quantitation of the accessible silanol population as a function of dehydration temperature on Aerosil 200 and Sylopol 952 silicas [50]

	accessible surface OH groups (OH/nm^2)					
	25°C	100°C	200°C	300°C	400°C	500°C
Aerosil 200	1.91		2.60			1.45
Sylopol 952	3.05	3.07	3.03	2.64	2.18	1.72

studies. Commercial supports are more likely to be the one of the economical silica gels, discussed in the next section.

1.4.2.2 Sylopol 952

The Sylopols are a family of silica gels manufactured by Grace Davison (Columbia, MD). These gels are made by acidifying a basic solution of sodium silicate. Once the gel is aged for an appropriate time, it is fed to a spray dryer to form the particles. Many factors may be varied to affect the initial micelle size and thus the end gel properties. The classification of the material (952, 955, 948 etc.) is based on isolation of different fractions to obtain the desired particle size distribution. Sylopol 952 is one of these gels with a surface area of 309 m^2/g, a pore volume of 1.61 mL/g and an average particle size of 112 μm. Its pH value is ca. 7.0. The pore size distribution of Sylopol 952, **Figure 1.5**, reveals that approx. 90% of the pores are in the range 5-30 nm, i.e., as micropores and mesopores, while macropores (>50 nm) contribute less than 5%. The micropores are likely the location of the inaccessible hydroxyls. Silanol groups exist both free and hydrogen-bonded.

Porous silica gels have rugged surfaces. Avnir et al.[51] reported that the surface of Sylopol 952 has a fractal exponent close to 3.0. Therefore, the surface is highly irregular and self-similar over a certain range of scale. **Figure 1.6** depicts the rugged surface of a silica gel surface. Although a random distribution of hydroxyls is

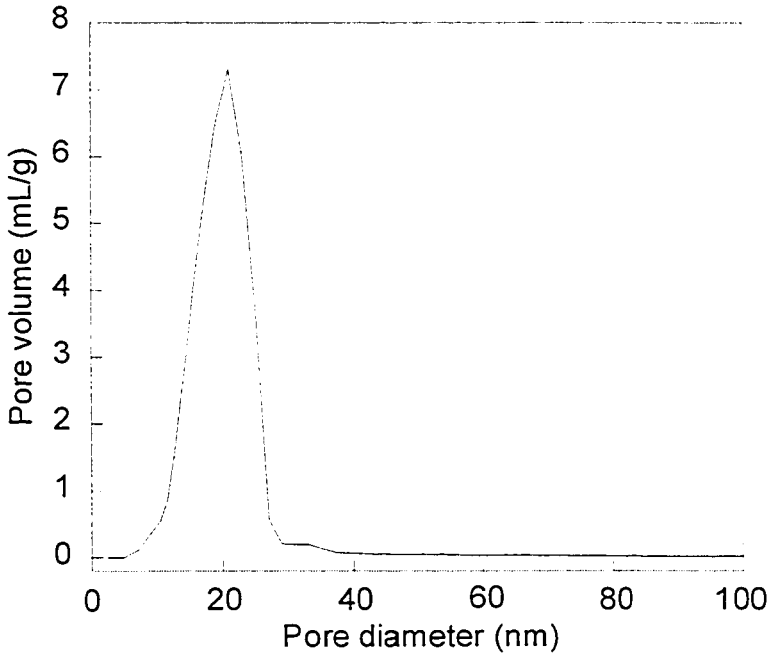

Figure 1.5 Pore size distribution of Sylopol 952 silica.

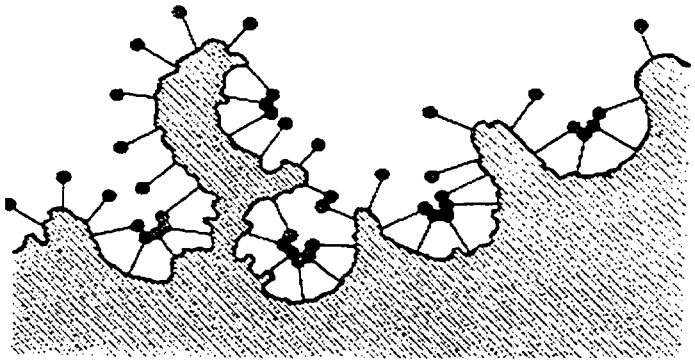

Figure 1.6 Rugged surface model (solid points represent silanol groups).[52]

assumed, clustering naturally occurs in the pores.

FTIR spectra of Sylopol silica show the O-H stretch of free silanols at 3747 cm^{-1} and H-bonded silanols at 3700-3200 cm^{-1}, **Figure 1.3**. Compared with Aerosil 200, hydrogen-bonded silanols are more abundant on Sylopol 952. The density of accessible silanol groups is also greater on Sylopol 952 than on Aerosil 200, **Table 1.2**, although the same trend of decreasing hydroxyl content as the temperature increases pertains.

1.5 References

(1) Whyman, R. *Appl. Organomet. Chem. Catal.* **2001**, *96*, 58-76.

(2) Morse, P. M. *Chem. Eng. News*, May 24, 1999, 11-17.

(3) Cossee, P. *J. Catal.* **1964**, *3*, 80.

(4) Ivin, K. J.; Rooney, J. J.; Stewart, C. D.; Green, M. L. H.; Mahtab, R. *J. Chem. Soc., Chem. Commun.* **1979**, 604-606.

(5) Dawoodi, Z.; Green, M. L. H.; Mtetwa, V. S. B. Prout, K. *J. Chem. Soc., Chem. Commun.* **1982**, 1410-1411.

(6) Laverty, D. T.; Rooney, J. J. *J. Chem. Soc., Farad. Trans. 1* **1983**, *79*, 869-878.

(7) Brookhart, M.; Green, M. L. H. *J. Organomet. Chem.* **1983**, *250*, 395-408.

(8) Brookhart, M.; Green, M. L. H.; Wong, L. L. *Prog. Inorg. Chem.* **1988**, *36*, 1-124.

(9) Theopold, K. H. *CHEMTECH* **1997**, 26-32.

(10) McDaniel, M. P. *Adv. Catal.* **1985**, *33*, 47.

(11) Weckhuysen, B. M.; Schoonheydt, R. A. *Catal. Today* **1999**, *51*, 215.

(12) Weckhuysen, B. M.; Wachs, I. E.; Schoonheydt, R. A. *Chem. Rev.* **1996**, *96*, 3327.

(13) Krauss, H. L.; Hagen, K.; Hums, E. *J. Mol. Catal.* **1985**, *28*, 233-238.

(14) McDaniel, M. P. *Adv. Catal.* **1985**, *33*, 47-98.

(15) Candlin, J. P.; Thomas, H. *Adv. Chem. Ser.* **1974**, *132*, 212-239.

(16) Eley, D. D.; Rochester, C. H.; Scurrell, M. S. *Proc. Royal Soc. Ser. A* **1972**, *329*, 361.

(17) Freundlich, J. S.; Schrock, R. R.; Cummins, C.C.; Davis, W. M. *J. Am. Chem. Soc.* **1994,** *116*, 6476-6477.

(18) Giannini, L.; Solari, E.; Floriani, C.; Chiesi-Villa, A.; Rizzoli, C. *J. Am. Chem. Soc.* **1998**, *120*, 823-824.

(19) Ghiotti, G.; Garrone, E.; Coluccia, S.; Morterra, C.; Zecchina, A. *J. Chem. Soc., Chem. Commun.* **1979**, 1032-1033.

(20) Al-Mashta, F.; Davanzo, C. U.; Sheppard, N. *J. Chem. Soc., Chem. Commun.* **1983**, 1258-1259.

(21) McDaniel, M. P. *Adv. Catal.* **1985**, *33*, 47-98.

(22) Hogan, J. P. *J. Polym. Sci.: A-1* **1970**, *8*, 2637-2652.

(23) Espenson, J. H. Chemical Kinetics and Reaction Mechanisms; McGraw-Hill: New York, 1981.

(24) Basset, J. M.; Gates, B. C.; Candy, J.-P.; Choplin, J.; Leconte, M.; Quignard, F.; Santini, C. *Surface Organometallic Chemistry: Molecular Approaches to Surface Catalysis;* Kluwer: Dordrecht, 1988.

(25) Basset, J. M.; Choplin, J. *J. Mol. Catal.* **1985**, *21*, 95.

(26) Carrick, W. L.; Turbett, R. J.; Karol, F. J.; Karapinka, G. L.; Fox, A. S.; Johnson, R. N. *J. Polym. Sci.:A-1* **1972**, *10*, 2609-2620.

(27) Yermakov, Y.; Zakharov, V. *Adv. Catal.* **1975**, *24*, 173-219.

(28) Scott, S. L.; Basset, J. M.; Niccolai, G. P.; Santini, C.C.; Candy, J. P.; Lecuyer, C.; Quignard, F.; Choplin, A. *New J. Chem.* **1994**, *18*, 115-122.

(29) McCarthy, D. W.; Mark, I. E.; Schaefer, D. W. *J. Polym. Sci., B: Polym. Phys.* **1998**, *36*, 1167-1189.

(30) Choi, S.-S. *J. Appl. Polym. Sci.* **2001**, *79*, 1127-1133.

(31) Gorte, R. J. *Catal. Lett.* **1999**, *62*, 1-13.

(32) de Gauw, F. J. M. M.; van Santen, R. A. *Stud. Surf. Sci. Catal.* **2000**, *130A*, 127-135.

(33) Fink, G.; Steinmetz, B.; Zechlin, J.; Przybyla, C.; Tesche, B. *Chem. Rev.* **2000**, *100*, 1377-1390.

(34) Hlatky, G. G. *Chem. Rev.* **2000**, *100*, 1347-1376.

(35) Heaney, P. J.; Prewitt, C. T.; Gibbs, G. V. *Silica: Physical Behavior, Geochemistry and Materials Applications;* Mineralogical Society of America: Washington, D. C., 1994.

(36) Dijkstra, T. W.; Duchateau, R.; van Santen, R. A.; Meetsma, A.; Yap, G. P. A. *J. Am. Chem. Soc.* **2002**, *124*, 9856-9864.

(37) Iler, R. K. *The Chemistry of Silica*; Wiley: New York, 1979; Chapter 6.

(38) Snyder, L. R. *Principles of Adsorption Chromatography;* Dekker: New York, 1968.

(39) Guiochon, G.; Shirazi, S. G.; Katti, A. M. *Fundamentals of Preparative and Nonlinear Chromatography;* Academic Press: New York, 1994.

(40) Nawrocki, J. *J. Chromatogr., A* **1997**, *779*, 29-71.

(41) Tan, L. C.; Carr, P. W.; Abraham, M. H. *J. Chromatogr., A* **1996**, *752*, 1-18.

(42) Brinker, C. J.; Scherer, G. W. *Sol-Gel Science: The Physics and Chemistry of Sol-Gel Processes*; Academic Press: New York, 1990.

(43) Bergna, H. E. *The Colloid Chemistry of Silica*, *Adv. Chem. Ser. 234*; American Chemistry Society: Washington, DC, 1994.

(44) Ong, S. W.; Zhao, X. L.; Eisenthal, K. B. *Chem. Phys. Lett.* **1992**, *191*, 327-335.

(45) Iler, R. K. *The Chemistry of Silica*; Wiley: New York, 1979, Chapter 6.

(46) Peri, J. B.; Hensley, A. L.; *J. Phys. Chem.* **1968**, *72*, 2926-2933.

(47) Mathias, J.; Wannemacher, G. *J. Colloid Interface Sci.* **1988**, *125*, 61-68.

(48) Avnir, D.; Farin, D. *Nature* **1984**, *308*, 261.

(49) Product Information provided by Degussa-Hüls, NJ, USA.

(50) Taha, Z. A.; Scott, S. L. manuscript in preparation.

(51) Avnir, D.; Farin, D.; Pfeifer, P. *New J. Chem.* **1992**, *16*, 439-449.

(52) Tuel, A,; Hommel, H.; Legrand, A. P.; Chevallier, Y.; Morawski, J. C. *Colloids Surf.* **1990**, *45*, 413-426.

Chapter 2

Experimental Techniques

2.1 Reagents

2.1.1 Solid oxide supports

Two types of silicas were used as the oxide supports in these experiments. Pyrogenic Aerosil 200 is manufactured by Degussa Corporation AG (Frankfur, FRG).[1] This amorphous silica has a surface area in the range 175-225 m^2/g. The primary particles are nonporous with an average size (by TEM) of 12 nm. The silica gel Sylopol 952 is produced by Grace Davison. Sylopol 952 has a surface area of 309 m^2/g, a pore volume of 1.61 mL/g and an average particle size of 112 μm.

2.1.2 Commercial reagents and solvents

Reagents purchased for this research were of the highest purity level commercially available. Styrene (+99.0%, Aldrich) was stored in a glass reactor over molecular sieves. Before use, it was subjected to several freeze-pump-thaw cycles in order to remove dissolved gases. Styrene vapour was introduced into the experimental

reaction vessel via a high vacuum manifold. $(CH_3)_3SiCH_2MgCl$ (1 M in diethyl ether), neopentyl bromide (98%), 1-hexene (+99%), neohexene (95%) and 4,4-dimethyl-1-pentene (99%) were used as received from Aldrich. Mg (Aldrich) was oven-dried at 150°C for 24 hours before use. The solvent hexane (98.5%) was purified by column purification prior to use.

NaOH, KOH and Na_2CrO_4 were used as received from AnalaR. H_2O_2 (30% solution, GR. ACS, Merck KGaA) was used as received.

2.1.3 Gases

Ethylene (99.99%), propylene (99.6%) and HCl (99.5%), from Matheson Gas Products, were purchased in gas cylinders. Neopentane (+96%) in a lecture bottle was transferred into a glass bulb before use.

Ethylene and propylene had to be highly pure to avoid decomposing the catalysts. To remove water and O_2, a trap containing 4Å molecular sieves (Fisher Scientific Co.) and BTS-Catalyst (Fluka Chemica) was activated under a flow of H_2 at 250°C for 4 hours, followed by heating at 250°C under dynamic vacuum for 3 hours. The gases were passed through this trap into their storage bulbs, which were also equipped with 4Å molecular sieves.

2.2 Synthesis of molecular Cr(IV) precursors

The preparation of tetraalkylchromium(IV) complexes, CrR_4, (R = neopentyl, neosilyl) was accomplished by the interaction of Grignard or lithium reagents with the tetrahydrofuran adduct of chromic chloride, $CrCl_3 \cdot 3THF$.[2,3,4]

2.2.1 $Cr(CH_2C(CH_3)_3)_4$

Oven-dried magnesium (1.1 g, 45 mmol) was introduced into a 3-necked flask connected to a Schlenk line under a nitrogen atmosphere. After evacuating the system overnight, 25 mL dry diethyl ether was added and the mixture was stirred for half an hour at room temperature. Under nitrogen, 5.0 g (33 mmol) neopentyl bromide was introduced via a dropping funnel. The mixture was stirred and refluxed for 18 hours at room temperature. The remaining magnesium at this point was a small amount of dark gray scraps left over from the initial light gray metal fillings. The color change of the mixture from colorless to gray-green indicated the success of the reaction, equation 2.1.

$$(CH_3)_3CCH_2Br + Mg \rightarrow (CH_3)_3CCH_2MgBr \qquad (2.1)$$

The solution was transferred through a cannula into a Schlenk tube under N_2. The Grignard reagent $(CH_3)_3CCH_2MgBr$ in ether was thus obtained and stored in the Schlenk tube at -18°C.

The concentration of the Grignard reagent was determined by back-titration in a 50 mL Schlenk tube under N_2. 1 mL of the solution was introduced, then treated with an excess of 0.1 M HCl (15 mL). The mixture was back-titrated with 7.8 mL NaOH (0.1 M) using phenolphthalein to indicate the endpoint. This resulted in a concentration of $(CH_3)_3CCH_2MgBr$ of 0.72 M in diethyl ether, for a yield of 76%.

To a stirred suspension of $CrCl_3 \cdot 3THF$ (1.6 g, 4.3 mmol) in diethyl ether, the solution of $(CH_3)_3CCH_2MgBr$ (25 mL, 18.0 mmol) was added dropwise at room temperature over 10 minutes. The purple mixture was allowed to stir for one hour until it turned to a deep maroon color, indicating the presence of $Cr(CH_2C(CH_3)_3)_4$, equation 2.2.

$$6\ (CH_3)_3CCH_2MgBr + 2\ CrCl_3 \cdot 3THF \rightarrow Cr(CH_2C(CH_3)_3)_4 + Cr(CH_2C(CH_3)_3)_2 + 6\ MgBrCl + 6\ THF \qquad (2.2)$$

The solvent was removed under vacuum to a cold trap. Then 50 mL dry hexane was added to the solid residue and the mixture was stirred for half an hour. After filtering through a frit under N_2, the procedure was repeated and the solvent was evaporated. The deep maroon solid was purified by tube-to-tube sublimation

under high vacuum. Pure $Cr(CH_2C(CH_3)_3)_4$ was thus obtained in a yield of 33%. $Cr(CH_2C(CH_3)_3)_4$ is extremely air and moisture-sensitive and was stored under nitrogen in the freezer.

2.2.2 $Cr(CH_2Si(CH_3)_3)_4$

60 mL $(CH_3)_3SiCH_2MgCl$ (50 mmol, 0.83 M in diethyl ether) and 5.2 g (14 mmol) $CrCl_3 \cdot 3THF$ were used in the same procedure as for preparing $Cr(CH_2C(CH_3)_3)_4$. The yield of purple $Cr(CH_2Si(CH_3)_3)_4$ was 45 %.

2.3 Preparation of silica-supported Cr(IV)

2.3.1 Pretreatment of silica

In order to ensure reproducibility, silica was pretreated following a standard procedure. Pellets of Aerosil 200 silica were made from 8-30 mg silica by pressing at 125 kg/m^2 into a self-supporting disk of diameter 1.6 cm. The disk was placed in a sample holder inserted into an IR cell, **Figure 2.1(a)**. Sylopol 952 silica pellets were made in the same manner but with 15-40 mg silica and higher pressure (375 kg/m^2). For the powdered silica samples, both silicas were compacted by pressing thick pellets which were then ground in a mortar.

Silica was placed in an IR reactor for thermal treatment at 200°C under dynamic vacuum (<10^{-4} Torr) for a minimum of four hours. These thermal treatments do not change the surface area of the silica but they do remove adsorbed water and standardize the number of surface silanol groups.

2.3.2 Sublimation grafting

The breakseal reactor, **Figure 2.1(b)**, is used to protect fragile chromium precursors from air and moisture during experiments. The chromium complex was sublimed from its Schlenk storage tube into the breakseal reactor via a U tube with the aid of a liquid N_2 trap. After ca. 48 hours, the amount of compound is usually enough for a single experiment. The breakseal reactor was isolated under static vacuum. It was then carefully sealed along the pre-made restriction using a torch while the chromium compound was completely submerged in liquid nitrogen. A "hammer" consisting of a nail sealed inside a glass rod was placed on the opposite side of the breakseal and held in place with a magnet. A new restriction was made on the other side of the "hammer" to facilitate sealing after completion of grafting. The open end of the breakseal was then welded to the IR cell using a torch.

After breaking the breakseal with the "hammer", the organochromium compound was sublimed *in vacuo* at room temperature onto the thermally treated silica pellet.

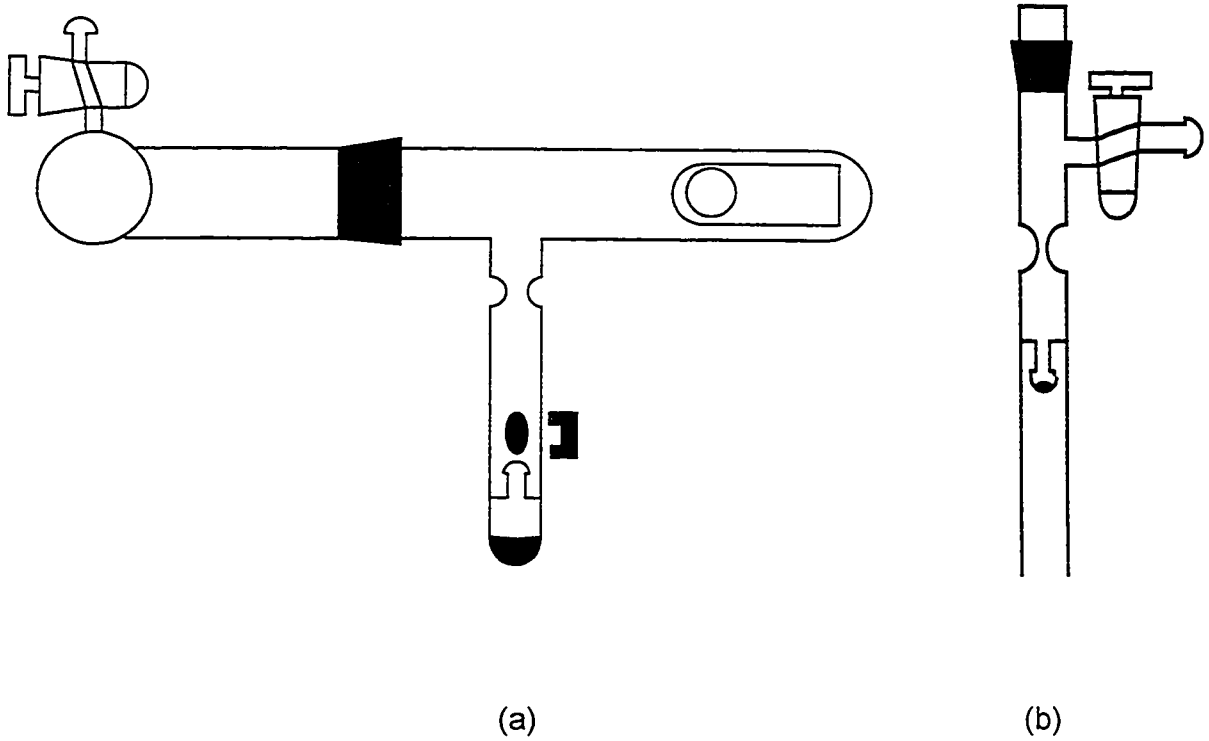

Figure 2.1 Schematics of (a) an IR cell; (b) a breakseal reactor.

The pellet holder was displaced in the IR cell to the region of the breakseal in order to allow chemisorption occur. After grafting, physisorbed material was removed from the reactor by submerging the breakseal in liquid nitrogen and sealing off the collected material at the restriction.

2.3.3 Solution grafting

100 mg Aerosil 200 was pressed and then ground to a coarse powder. The powder was placed in a stopcock-equipped Schlenk-type reactor to which had been attached a breakseal sidearm, with a restriction to facilitate sealing off. The silica was treated at 200°C under dynamic vacuum for four hours. In the glove box, ca. 3 mg $Cr(CH_2C(CH_3)_3)_4$ was dissolved in 200 mL dry hexane in a Schlenk tube and stirred for 20 minutes. The maroon solution was transferred into the reactor containing the silica. The suspension was stirred gently at room temperature for four hours and the solution remained colored during the process.

After grafting, the silica was allowed to settle and the supernatant was removed by cannula. The solid was washed with 100 mL freshly dried hexane and stirred for 20 minutes to remove physisorbed chromium from the silica. After removing most of the washing solvent via cannula, the rest was removed to a liquid nitrogen cold trap followed by three hours of high vacuum evacuation to complete the drying. The reactor

was isolated from the high vacuum line and the silica-supported chromium was transferred into the breakseal, which was then sealed off at the restriction.

2.4 IR characterization

Infrared experiments were performed in a high vacuum *in situ* IR reactor equipped with KCl windows (International Crystal Labs), capable of holding static vacuum (10^{-4} Torr) for four days. Transmission infrared spectra were recorded on a Mattson Research Series FTIR spectrometer equipped with a DTGS detector and purged with CO_2-free dry air. Background and solid sample spectra were recorded by co-adding 32 scans at a resolution of 2 cm^{-1}, while gas phase spectra were recorded at a resolution of 0.75 cm^{-1}. In recording IR spectra of the pellet, sample scans were taken by moving the sample holder within the reactor so that the pellet was aligned with the KCl windows perpendicular to the IR beam. To record gas phase IR spectra, the sample holder was slid back and out of the beam so that the IR windows presented an unobstructed view of the gas phase inside the cell.

2.5 Elemental analysis

Quantitation of the Cr loading was achieved by extraction of the metal from the modified silica at the end of each experiment for analysis by UV-Vis. A calibration

curve was prepared using Na_2CrO_4 (20-200 μM), **Figure 2.2.** All spectra were recorded in quartz cuvettes with 1 cm path length referenced to the $NaOH/H_2O_2$ solution. To extract Cr from silica, 5 mL 5 M NaOH was added followed by 1 mL 30% H_2O_2 to ensure complete oxidation of Cr(IV) to Cr(VI). The yellow solution was boiled for two hours to destroy unreacted H_2O_2 and diluted to 50 mL with distilled water to produce a Cr concentration of ca. 50 μM. CrO_4^{2-} has a maximum absorbance at λ=376 nm. The concentration of Cr in the sample was obtained by measuring the absorbance at 376 nm and comparing it to the calibration curve.

2.6 Quantitation of NpH

Quantitative analysis of neopentane liberated in thermolysis of $(\equiv SiO)_2Cr(CH_2C(CH_3)_3)_2$ was determined by comparison of the intensity in the ν(CH) region (2960 cm^{-1}) of the gas phase IR spectrum with an infrared calibration curve constructed using pure neopentane, **Figure 2.3**. The gas phase IR cell has a pathlength of 7 cm.

2.7 Gas phase GC analysis

Gas chromatographic analysis of gaseous products was performed isothermal at 40 ± 0.5 or 50 ± 0.5°C (depending on the number of carbons present in the

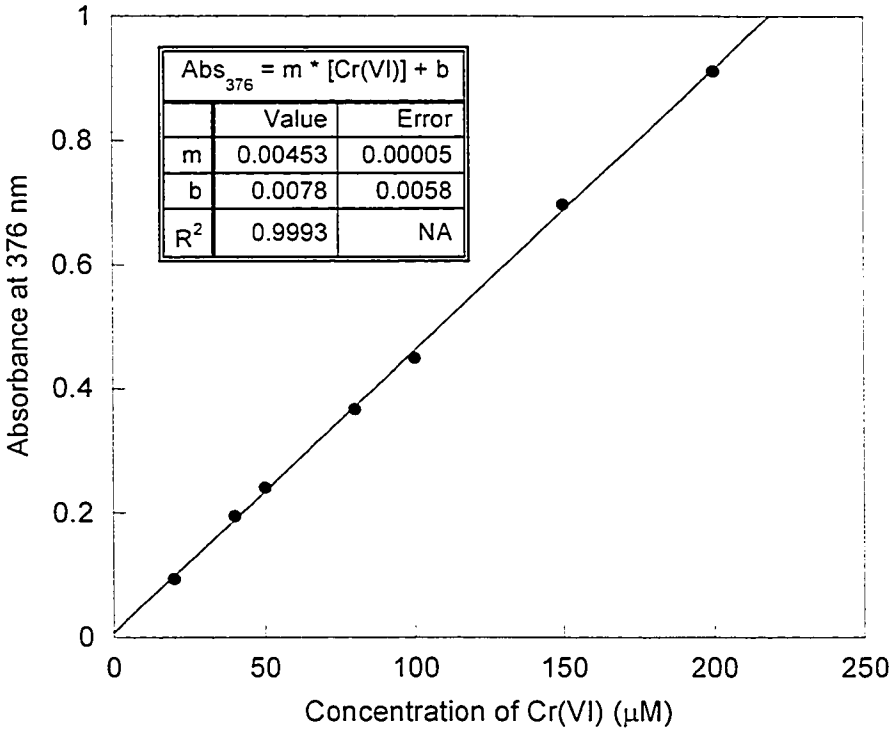

Figure 2.2 UV calibration curve for chromium analysis.

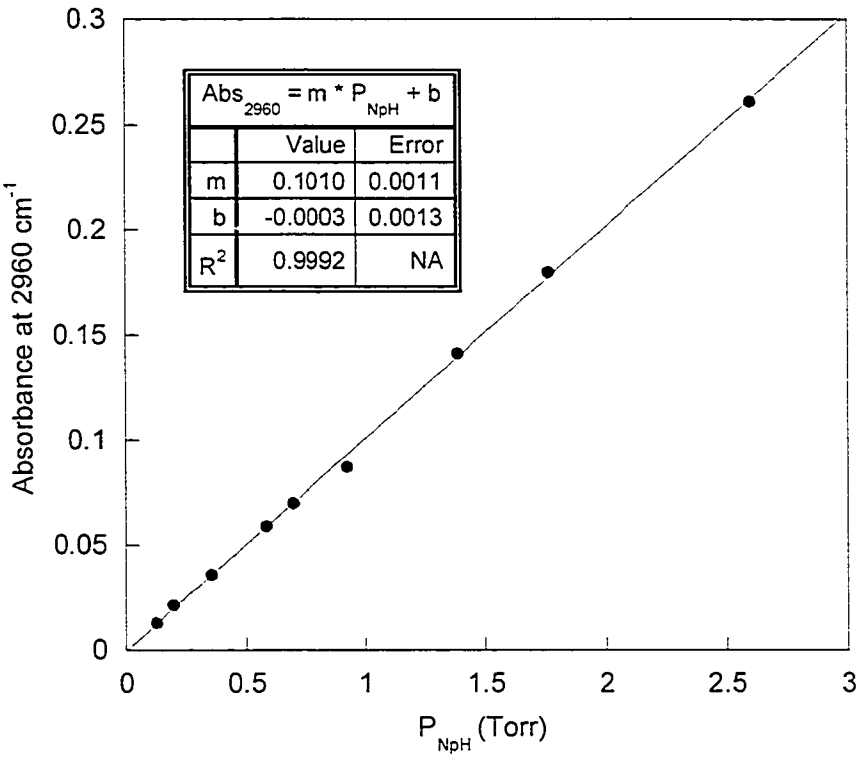

Figure 2.3 IR calibration curve for neopentane(g).

hydrocarbon) on a HP 6890A GC equipped with HP-5 column (30 m long x 0.320 mm i.d.), and with an FID detector. The identities of gases were determined by comparison to the retention times of standards under the same conditions.

2.8 Kinetics experiments

Kinetics measurements were made for the thermolysis of $(\equiv SiO)_2Cr(CH_2C(CH_3)_3)_2$ and in olefin polymerization. In both cases, gas phase IR spectra above the silica were recorded at regular time intervals. The IR cell was aligned in the IR spectrometer to ensure that the beam sampled the gas phase without passing through the solid. The amount of product (neopentane or olefin) in the gas phase was determined by the integration of the ν(CH) region to give the parameter A_t. Non-linear least-square fits with three variable parameters (A_0, $A\infty$, and k) were then used to fit the data. Equation 2.3 applies to thermolysis kinetics and equation 2.4 to olefin polymerization kinetics.

$$A_t = A\infty + (A_0 - A\infty)(e^{-kt}) \quad (2.3)$$

$$A_t = A_0 + (A\infty - A_0)(e^{-kt}) \quad (2.4)$$

In thermolysis experiments, a tube furnace with a thermocouple (±1 K) was placed around the bottom of the IR cell where the modified silica was located. The evolution of the neopentane liberated by thermolysis of $(\equiv SiO)_2Cr(CH_2C(CH_3)_3)_2$ was monitored at regular time intervals. In the case of olefin polymerization kinetics, a known pressure of olefin was introduced into the IR through the gas manifold and immediately condensed into a sidearm with a liquid nitrogen cold bath to prevent the reaction from being initiated. The reactor was moved to the IR spectrometer, the liquid nitrogen bath removed and spectra of the gas phase recorded. Polymerization reactions using powdered silica were performed at constant temperature by immersing the sidearm of an IR cell in a 22 °C water bath.

2.9 References

(1) Mathias, J.; Wannemacher, G. *J. Colloid Interface Sci.* **1988**, *125*, 61-68.

(2) Mowat, W.; Shortland, A.; Yagupsky, G.; Hill, N. J.; Yagupasky, M.; Wilkinson, G. *J. Chem. Soc., Dalton Trans.* **1972**, 533-542.

(3) Mowat, W.; Shortland, A.; Hill, N. J.; Wilkinson, G. *J. Chem. Soc., Dalton Trans.* **1973**, 770-778.

(4) Amor Nait Ajjou, J. Ph.D. thesis, University of Ottawa, 2000.

Chapter 3

Surface Chemistry of Tetraalkylchromium(IV) on Silicas

3.1 Introduction

The nature of the interaction between organometallic complexes and the surface of partially dehydroxylated silicas was first investigated in the early 1970's.[1] Generally, preparation of surface organometallic fragments can be accomplished by either sublimation of a volatile organometallic compound (i.e., gas-solid reaction) or solution impregnation of a non-volatile one (i.e., solution-solid reaction). In a limited number of cases, both techniques have been employed with the same organometallic compound. For example, Basset et al.[2] sublimed $Zr(CH_2C(CH_3)_3)_4$ onto Aerosil 200 silica pretreated at 500°C (referred to as A_{200}-500) and obtained the surface organometallic fragment $(\equiv SiO)Zr(CH_2C(CH_3)_3)_3$. Earlier, Schwartz et al.[3] had successfully synthesized the surface organometallic fragment $(\equiv SiO)Zr(CH_2C(CH_3)_3)_2$ on Aerosil 200 silica pretreated at 200°C (referred to as A_{200}-200) by impregnation with a toluene solution of $Zr(CH_2C(CH_3)_3)_4$. It has not been established whether, if one uses the same type of silica, these two methods of grafting give the same product.

A consideration which bears on the feasibility of different grafting methods is the origin of the driving force for chemisorption. The driving force, or the Gibbs free energy, consists of contributions from both enthalpy and entropy which together

determine the spontaneity of a reaction. Grafting reactions presumably have similar enthalpies whether they are achieved by sublimation or solution grafting. However, the entropy contribution, $-T\Delta S$, to the driving force is greater during the process of sublimation than during solution grafting if a volatile reaction product is formed. In the examples described above, the neopentane liberated by sublimation grafting, equation 3.1, has more entropy than the solvated $C(CH_3)_4$ liberated by solution grafting, equation 3.2.

$$\equiv SiOH + Zr(CH_2C(CH_3)_3)_4(g) \rightarrow (\equiv SiO)Zr(CH_2C(CH_3)_3)_3 + C(CH_3)_4(g) \quad (3.1)$$

$$2 \equiv SiOH + Zr(CH_2C(CH_3)_3)_4(solv.) \rightarrow (\equiv SiO)_2Zr(CH_2C(CH_3)_3)_2 + 2\ C(CH_3)_4\,(solv.) \quad (3.2)$$

Some grafting reactions are clearly driven by entropy. For example, $VOCl_3(g)$ reacts quickly and completely with the surface hydroxyl groups of A_{200}-500, yet very little reaction occurs when silica is stirred with solution of $VOCl_3$ in toluene.[4] There is no reaction between $Cr(CH_2C(CH_3)_3)_4$ and water or alcohols. However, sublimation of $Cr(CH_2C(CH_3)_3)_4$ onto silica does result in reaction with the surface hydroxyl groups, equation 3.3.[5] Neopentane is liberated to the gas phase, where it contributes to the reaction entropy.

$$n \equiv SiOH + Cr(CH_2C(CH_3)_3)_4 \rightarrow (\equiv SiO)_nCr(CH_2C(CH_3)_3)_{4-n} + n\ C(CH_3)_4(g) \quad (3.3)$$

If this grafting is favorable only because of the entropy term, then no reaction is expected using the solution grafting technique. However, if the enthalpy is also favorable, then solution grafting should be possible.

The average stoichiometry of the grafting reaction depends on the density and distribution of silanol groups on the partially dehydroxylated silica surface. Attempts to characterize surface organometallic complex(es) have led previous researchers to suggest that *mixtures* of surface species are always produced. This made it difficult to draw unambiguous conclusions about the reactivity of individual organometallic fragments. However, previous research in the Scott group revealed that surface organochromium(IV) complexes are uniform rather than mixtures.[5] In that study, the support used was Aerosil 200 manufactured by Degussa. It is a good model support for surface chemistry research because it is nonporous, flat and since it is prepared by fuming $SiCl_4$, very pure. A clean surface reaction was reported on this model support, equation 3.4:

$$2\ \equiv SiOH\ +\ Cr(CH_2C(CH_3)_3)_4\ \rightarrow\ (\equiv SiO)_2(CH_2C(CH_3)_3)_2\ +\ 2\ C(CH_3)_4 \qquad (3.4)$$

where the average stoichiometry is also the exact stoichiometry of grafting.

Degussa Aerosils are expensive silicas. In real catalyst synthesis, the supports employed are relatively cheap silica gels. These porous materials have more complex structures than the Aerosils. However, their porosity contributes to their activity

because fracturing of the catalyst during polymerization exposes fresh active sites and reduces the size of the catalyst particles which remain in the polymer after reaction. A family of industrial supports is the Sylopols made by Grace. In this chapter, Sylopol 952 will be employed to investigate the surface chemistry of $Cr(CH_2C(CH_3)_3)_4$, in order to demonstrate whether the grafting stoichiometry observed on Aerosil is also obtained on the porous support, as well as how the nature of the silica influences subsequent surface chemistry such as the thermal transformation of the bis(neopentyl)chromium(IV) fragment to the corresponding neopentylidene.

3.2 Grafting of $Cr(CH_2C(CH_3)_3)_4$ on Aerosil 200 by sublimation

3.2.1 Pretreatment of Aerosil silica

A standard pretreatment protocol was used to ensure reproducible surface chemistry on Aerosil 200 silica. The density of overall surface hydroxyl groups (accessible and inaccessible) is determined by the temperature at which the silica surface is treated. In this research, Aerosil 200 silica was typically subjected to thermal treatment at 200°C under dynamic vacuum. The condensation of neighboring hydroxyl groups produces a partially dehydroxylated silica surface. During this process, the density of surface hydroxyl groups decreases from 4.9 to 2.6 OH/nm^2.[6]

Aerosil 200 silica subjected to 200°C thermal treatment will be referred to as A_{200}-200 in this thesis.

FTIR spectroscopy of a self-supporting disk of silica reveals a band at 3747 cm^{-1} attributed to non-hydrogen-bonded surface OH groups, **Figure 3.1a**. A broad shoulder at ca. 3690 cm^{-1} is assigned to the hydrogen-bonded OH groups. These are inaccessible to chemical agents, and are possibly located in the bulk of the silica structure.[7]

Broad bands at 1977, 1868 and 1647 cm^{-1} are overtones and combinations of the intense Si-O-Si fundamental modes originating in the bulk of the silica and which are unchanged by any reactions on the surface which do not alter the internal structure of silica.

3.2.2 Nature of the grafting reaction

3.2.2.1 Stoichiometry of grafting

The reactions of partially dehydroxylated Aerosil 200 (A_{200}-200) with an excess of the molecular complexes $Cr(CH_2C(CH_3)_3)_4$, **1a**, and $Cr(CH_2Si(CH_3)_3)_4$,**1b**, are self-limiting. Observing strict exclusion of air and moisture, both reactions proceed

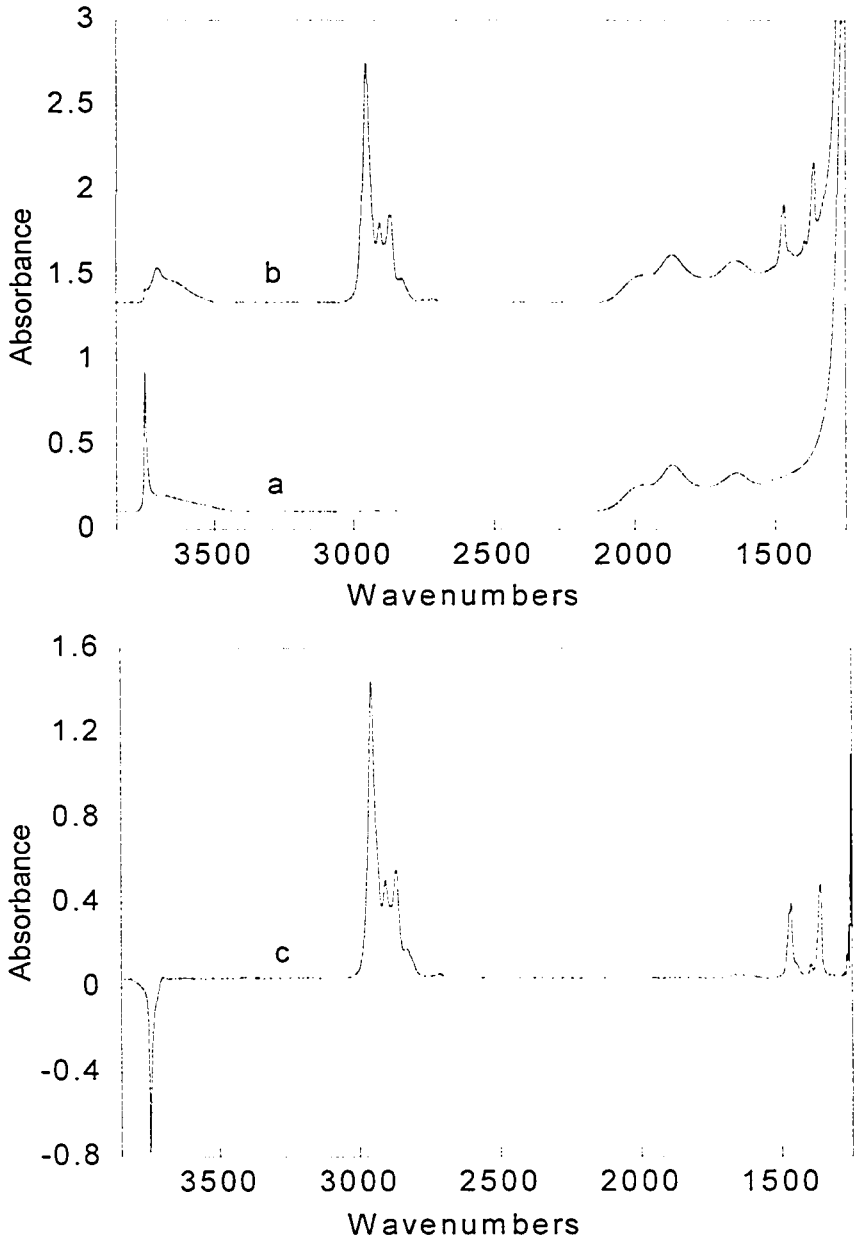

Figure 3.1 FTIR spectroscopy of a self-supporting disk of Aerosil 200: (a) partially dehydroxylated at 200°C; (b) after reaction with $Cr(CH_2C(CH_3)_3)_4$ (**1a**); (c) difference spectrum b-a.

quantitatively to give chemisorbed organochromium fragments on the silica surface. The grafting reactions are accompanied by evolution of a reproducible quantity of 2 equiv. neopentane for **1a** or tetramethylsilane (not quantified in this work) for **1b**. These are the only volatile products of sublimation grafting at room temperature. Neopentane was identified by GC-MS and FTIR spectroscopy. Quantitation of neopentane was achieved *in situ* by comparison of the gas phase absorbance at 2960 cm^{-1} to a calibration curve, **Figure 2.3**.

Cr was extracted and quantified spectrophotometrically as chromate. Neopentane yields and Cr contents for all grafting experiments on Aerosil 200 silica are summarized in **Table 3.1**. Based on the average of twelve experiments, (1.90±0.07) moles of neopentane are liberated per mole of grafted Cr on A_{200}-200, regardless of Cr loading in the range of 0.18-0.39 Cr/OH.

In order to investigate the composition and structure of the surface organochromium fragment, the grafted materials were deliberately subjected to protonolysis in three independent experiments. Treatment with excess HCl(g) caused the color to change from orange to green. The sole volatile product was identified as neopentane. The yield was determined as (1.87±0.06) NpH/Cr in three experiments, **Table 3.1**. Thus, the organochromium surface complexes have the composition $(\equiv SiO)_2Cr(CH_2C(CH_3)_3)_2$, formed with the overall grafting stoichiometry shown in equation 3.4 (section 3.1).

Table 3.1 Quantitative analysis of the products during grafting of $Cr(CH_2C(CH_3)_3)_4$ and subsequent protonolysis on Aerosil 200 silica

Grafting							Protonolysis	
mass of silica mg	Cr wt%	Cr μmol	OH [a] μmol	Cr/OH	NpH μmol	NpH/Cr	NpH μmol	NpH/Cr
8.2	0.82	1.3	7.1	0.18	2.4	1.85		
12.4	1.21	2.9	10.7	0.27	5.2	1.79	5.4	1.86
8.9	1.75	3.0	7.7	0.39	5.9	1.97		
11.1	1.51	3.2	9.5	0.34	5.7	1.78		
13.8	1.47	3.9	11.9	0.33	7.1	1.82		
14.9	1.36	3.9	12.8	0.30	7.3	1.87	7.0	1.79
12.5	1.71	4.1	10.8	0.38	8.0	1.95		
14.3	1.64	4.5	12.3	0.37	9.1	2.02		
15.1	1.58	4.6	13.0	0.35	8.7	1.89		
16.3	1.74	5.5	14.0	0.39	11.0	2.00	10.7	1.95
19.8	1.68	6.4	17.0	0.38	12.7	1.98		
28.6	1.29	7.1	24.6	0.29	13.8	1.94		
						Avg.1.90±0.07		Avg.1.87±0.06

[a] The number of surface hydroxyl groups initially present is calculated from the hydroxyl content of A_{200}-200 (0.86 mmol OH/g silica).[7]

The subsequent protonolysis reaction is described in equation 3.5.

$$(\equiv SiO)_2Cr(CH_2C(CH_3)_3)_2 + \text{excess HCl (g)} \rightarrow \text{“}(\equiv SiO)_2CrCl_2\text{”} + 2\ C(CH_3)_4 \quad (3.5)$$

The product $(\equiv SiO)_2CrCl_2$ was not characterized but is included to balance the reaction. These reactions are consistent with previous results reported by the Scott group.[5]

The reaction of **1b** with Aerosil silica surface was previously shown to proceed with the same grafting stoichiometry, equation 3.6.[5]

$$2 \equiv SiOH + Cr(CH_2Si(CH_3)_3)_4 \rightarrow (\equiv SiO)_2Cr(CH_2Si(CH_3)_3)_2 + 2\ Si(CH_3)_4 \quad (3.6)$$

3.2.2.2 IR characterization of supported neopentylchromium fragments

Characterization of the reactions of **1a** and **1b** with the surface of Aerosil 200 silica was carried out by *in situ* IR spectroscopy. When **1a** or **1b** is sublimed at room temperature in an *in situ* IR cell onto a self-supporting disk of A_{200}-200, the sharp band at 3747 cm^{-1} disappears completely, and is not regenerated when unreacted **1a** or **1b** are desorbed to a liquid N_2 trap, **Figures 3.1 and 3.2**. The broad shoulder at ca. 3690 cm^{-1} remains visible after the reaction, indicating that these hydrogen-bonded

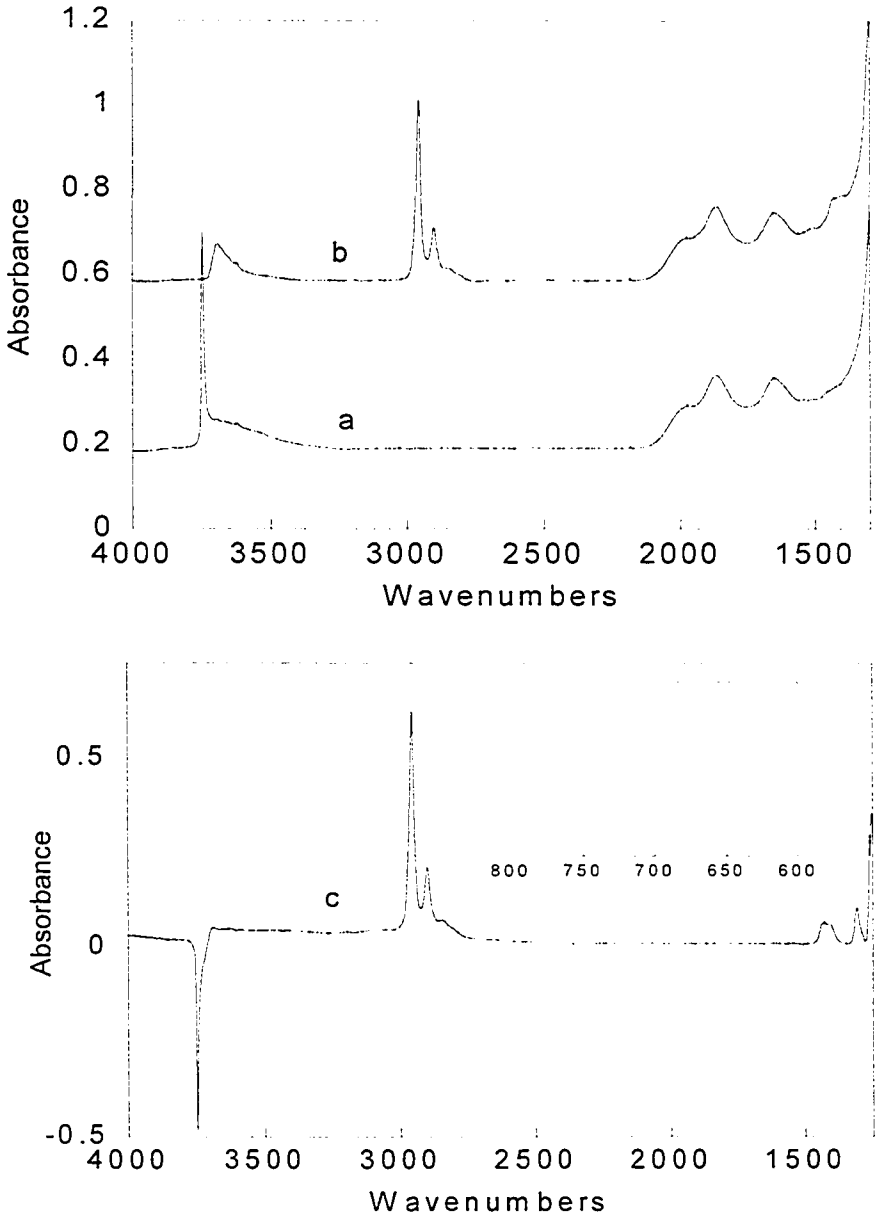

Figure 3.2 FTIR spectroscopy of a self-supporting disk of Aerosil 200: (a) partially dehydroxylated at 200°C; (b) after reaction with $Cr(CH_2Si(CH_3)_3)_4$ (**1b**); (c) difference spectrum b-a. The inset shows the region of partial transparency where rocking modes are located.

hydroxyls are inaccessible. In addition, new bands characteristic of alkyl vibrations appear, in the regions (1) 3000-2800 cm^{-1}, assigned to C-H stretching vibrations; (2) 1500-1300 cm^{-1}, assigned to methyl and methylene deformations; (3) 750-680 cm^{-1}, attributed to methyl rocking modes coupled to Si-C stretching in the case of **1b**.[8]

3.2.3 Thermolysis

3.2.3.1 Stoichiometry

The molecular complex $Cr(CH_2C(CH_3)_3)_4$ is reported to be thermally stable in hexane at 80°C for several days.[9] In contrast, bis(neopentyl)chromium supported on Aerosil 200 silica is unstable when heated. It undergoes a transformation within four hours at 68°C which results in a reproducible decrease in the integrated ν(C-H) intensity of 48±1%, and liberation of (0.92±0.08) equiv of neopentane per Cr as the only gas phase product, **Table 3.2**. Likewise, neopentane is liberated when the thermolyzed sample is exposed to 30 Torr HCl(g) at room temperature. This treatment leads to the formation of (0.90±0.03) equiv. NpH per Cr site, **Table 3.2**. These results are consistent with the previous characterization of the thermolysis reaction as α-H

Table 3.2 Quantitative analysis of products of thermolysis of $(\equiv SiO)_2Cr(CH_2C(CH_3)_3)_2$ and subsequent protonolysis on Aerosil 200 silica

			Thermolysis			Protonolysis	
mass silica mg	Cr wt.%	Cr μmol	% loss of surface ν(CH) [a]	NpH μmol	NpH/Cr	NpH μmol	NpH/Cr
8.9	1.75	3.0	50.1	2.7	0.90	-	-
13.8	1.47	3.9	46.8	3.2	0.82	3.4	0.87
12.5	1.71	4.1	47.1	3.6	0.88	3.8	0.92
15.1	1.58	4.6	47.5	5.0	1.09	-	-
			Avg. 48±1		Avg. 0.92±0.08		Avg. 0.90±0.03

[a] From integration of the ν(CH) region 3200-2800 cm^{-1} in the IR spectrum of the Cr-modified Aerosil 200 silica. The integrated absorbance is proportional to the number of neopentyl groups present on the surface.

abstraction leading to a neopentylidene complex, equations 3.7-3.8.

$$(\equiv SiO)_2Cr(CH_2C(CH_3)_3)_2 \xrightarrow{\Delta} (\equiv SiO)_2Cr{=}CHC(CH_3)_3 + C(CH_3)_4 \quad (3.7)$$

$$(\equiv SiO)_2Cr{=}CHC(CH_3)_3 + 2\ HCl \rightarrow \text{“}(\equiv SiO)_2CrCl_2\text{”} + C(CH_3)_4 \quad (3.8)$$

3.2.3.2 Kinetics

A kinetic study of the thermolysis of $(\equiv SiO)_2Cr(CH_2C(CH_3)_3)_2$ on $Aerosil_{200}$-200 silica was performed *in vacuo* at 78°C. IR spectra of the volatile product (neopentane) were recorded at regular time intervals. The integrated absorbance of the *in situ* gas phase IR spectrum in the ν(CH) region indicates the progress of the surface reaction as a function of time, **Figure 3.3**. The kinetics of thermolysis for a 15.7 mg pellet loaded with 1.34 wt.% Cr show first-order behavior. The curve fit yields k = (0.0075±0.0001) min^{-1} at 78°C. An independent kinetics study of a powdered sample (24.9 mg, 1.26 wt.% Cr) was undertaken in the same fashion and gave k = (0.0046±0.0002) min^{-1} at 69°C. These rate constants agree well with Eyring data previously reported by the Scott group,[10] **Figure 3.4**, consistent with the intramolecular formation of a supported neopentylidenechromium(IV) fragment.

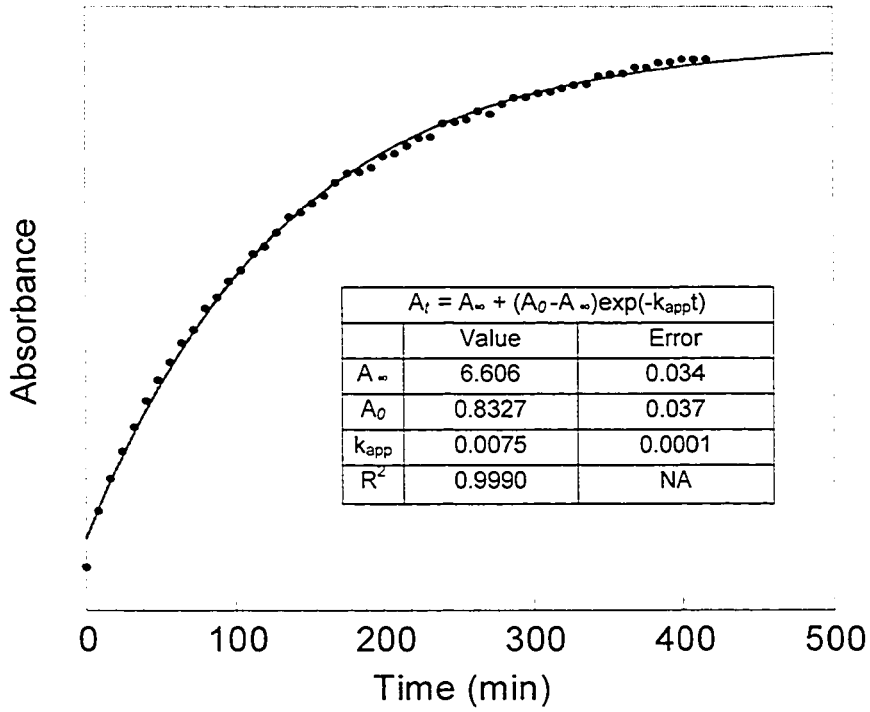

Figure 3.3 Time-resolved evolution of $C(CH_3)_4$ from $(\equiv SiO)_2Cr(CH_2C(CH_3)_3)_2$ on a 15.7 mg pellet of Aerosil 200 loaded with 1.34% wt.% Cr at 78°C, monitored as the integrated absorbance of the *in situ* gas phase IR spectrum in the ν(CH) region.

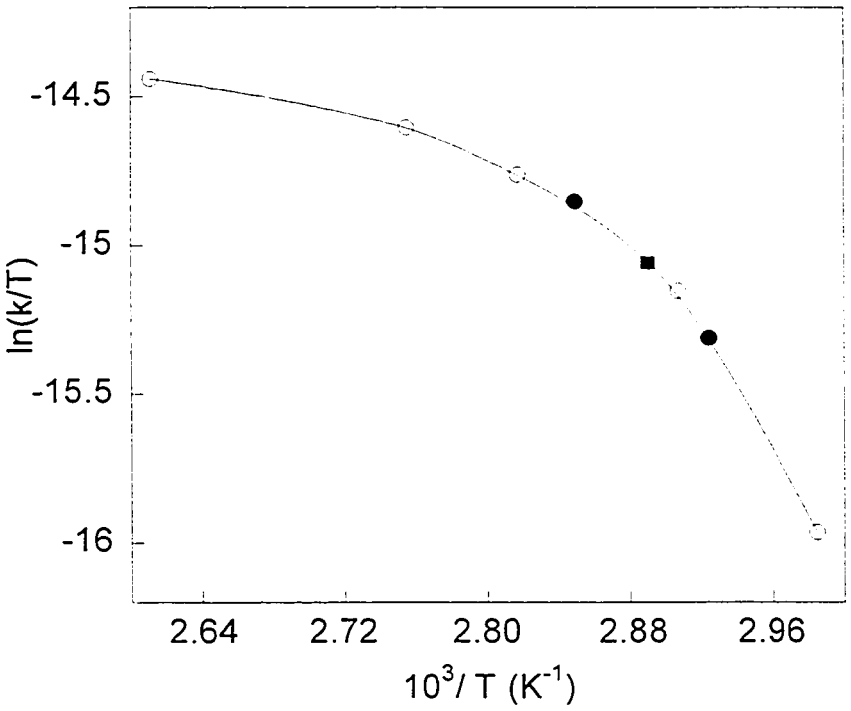

Figure 3.4 Comparison of rate constants for thermolysis of $(\equiv SiO)_2Cr(CH_2C(CH_3)_3)_2$ (solid circles, Aerosil 200; square, Sylopol 952) to previous Eyring data for Aerosil 200 (open circles).

3.2.3.3 Reactivity of Aerosil-supported neopentylidenechromium(IV)

NMR spectroscopic evidence for the alkylidene nature of the surface complex $(\equiv SiO)_2Cr{=}CHC(CH_3)_3$ is unavailable due to its paramagnetic nature. Therefore its characteristic reactivity towards the reagent $C_6H_5CH{=}CH_2$ was investigated.

Upon reaction of $(\equiv SiO)_2Cr{=}CHC(CH_3)_3$ with excess styrene vapor, $CH_2{=}CHC(CH_3)_3$ was identified by GC, by comparison to the retention time of a pure sample of neohexene. This is the expected product of olefin metathesis, equation 3.9.

$$(\equiv SiO)_2Cr{=}CHC(CH_3)_3 + C_6H_5CH{=}CH_2 \rightarrow$$
$$\text{“}(\equiv SiO)_2Cr{=}CHC_6H_5\text{”} + CH_2{=}CHC(CH_3)_3 \qquad (3.9)$$

The benzylidene complex was not further characterized but is included for completeness. This demonstrates the characteristic reactivity of a chromium alkylidene, consistent with previous conclusions about the nature of $(\equiv SiO)_2Cr{=}CHC(CH_3)_3$ from the Scott group.[11]

3.3 Grafting of $Cr(CH_2C(CH_3)_3)_4$ on Aerosil 200 by deposition from solution

3.3.1 Nature of the grafting reaction

Since sublimation of $Cr(CH_2C(CH_3)_3)_4$ is slow, the grafting procedure may be accelerated if $Cr(CH_2C(CH_3)_3)_4$ and silica are placed direct contact in a solvent. When 100 mg Aerosil 200 pretreated at 200°C was stirred with a solution of ca. 3 mg $Cr(CH_2C(CH_3)_3)_4$ in 200 mL hexane, the initially white silica powder became orange, the same color as the material prepared by sublimation grafting. After the experiment, Cr was extracted and the loading quantified to be 0.91 wt.%. For comparison, the maximum loading of $Cr(CH_2C(CH_3)_3)_4$ obtained by sublimation grafting in this research is 1.75 wt.% Cr.

3.3.2 Thermolysis

In order to verify that the materials obtained by sublimation and solution grafting are the same, their thermolytic behaviour was compared.

3.3.2.1 Stoichiometry

Neopentane was detected by *in situ* IR and GC as the only volatile product evolved from the supported chromium complex grafted from solution onto Aerosil 200 powder during its subsequent thermolysis at 68°C under vacuum for ca. 10 hours. The yield of NpH from a 90 mg sample was quantified as 14.3 μmol for a sample containing 15.8 μmol Cr, i.e., 0.9 NpH/Cr.

3.3.2.2 Kinetics

The time-resolved evolution of $C(CH_3)_4$ from $(\equiv SiO)_2Cr(CH_2C(CH_3)_3)_2$ grafted from solution onto Aerosil 200 silica is shown in **Figure 3.5**. A single exponential first-order curve fit with three variable parameters yielded the rate constant for thermolysis, $k(68°C) = (0.0042\pm0.0002)\ min^{-1}$. For comparison, the rate constant for thermolysis of $(\equiv SiO)_2Cr(CH_2C(CH_3)_3)_2$ prepared by sublimation grafting was found to be $(0.0046\pm0.0002)\ min^{-1}$ at 69°C (see section 3.2.3.2). Therefore we conclude that the materials prepared by grafting $Cr(CH_2C(CH_3)_3)_4$ onto Aerosil 200 by either sublimation or from solution are essentially the same.

3.4 Grafting of $Cr(CH_2C(CH_3)_3)_4$ on Sylopol 952 by sublimation

3.4.1 Pretreatment of silica surface

As with Aerosil 200, the temperature at which Sylopol 952 silica surface is treated determines its surface hydroxyl group content. At 200°C, the density of accessible hydroxyl groups on Sylopol 952 was measured to be 3.0 OH/nm^2,[4] compared to 2.6 OH/nm^2 on A_{200}-200. Sylopol 952 silica subjected to 200°C thermal treatment will be referred to as S_{952}-200 in this thesis. The IR spectrum of this material

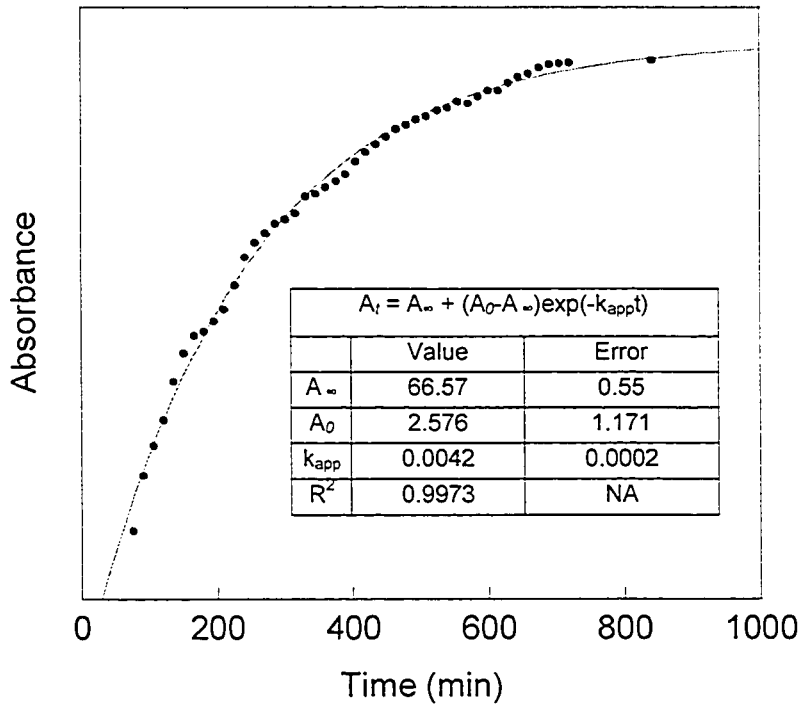

Figure 3.5 Time-resolved evolution of $C(CH_3)_4$ from solution-grafted $(\equiv SiO)_2Cr(CH_2C(CH_3)_3)_2$ at 68°C on 90 mg powdered Aerosil 200 silica with 0.91 wt.% Cr.

is shown in **Figure 3.6a**. Compared to the spectrum of A_{200}-200, **Figure 3.6b**, the OH band due to isolated hydroxyls is weaker and more hydroxyls are engaged in hydrogen-bonding. This is suggested to be a consequence of the porosity of Sylopol 952, which results in significant surface curvature, **Scheme 3.1**.[11]

Scheme 3.1 Schematic representation of hydroxyl-terminated surfaces of flat nonporous (Aerosil) and porous (Sylopol) silicas

Aerosil Sylopol

3.4.2 Nature of the grafting reaction

3.4.2.1 Stoichiometry of grafting

Grafting of $Cr(CH_2C(CH_3)_3)_4$ on $Sylopol_{952}$-200 was accomplished in the same fashion as the sublimation reaction on Aerosil 200. The same color change from white to orange was observed for both silicas.

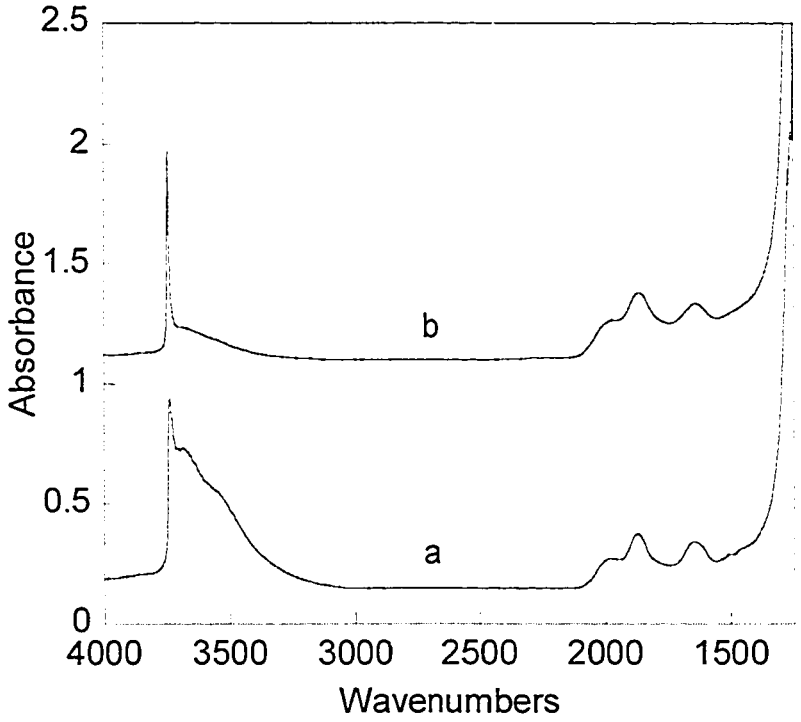

Figure 3.6 Comparison of FTIR spectra of self-supporting pellets of (a) S_{952}-200 and (b) A_{200}-200, both partially dehydroxylated at 200°C. The spectra have been normalized to the intensity of the SiOSi overtone at 1860 cm^{-1}.

On S_{952}-200, neopentane is the only gas phase product of grafting. Based on the results of seven experiments, (1.93±0.07) equiv. of neopentane is evolved per chemisorbed Cr regardless of the Cr loading in the range (1.04-2.31) wt.%, **Table 3.3**. Thus, the grafting stoichiometry on S_{952}-200 is the same as that on A_{200}-200, equation 3.4. Furthermore, the maximum loading of bis(neopentyl)chromium(IV) fragments achieved on S_{952}-200, 0.36 Cr/OH, is comparable to that on A_{200}-200, 0.39 Cr/OH (**Table 3.1**).

3.4.2.2 IR characterization of supported neopentylchromium fragments

The IR spectrum of the supported bis(neopentyl)chromium fragments on S_{952}-200 is shown in **Figure 3.7**. It is very similar to the spectrum on Aerosil silica (**Figure 3.1**), with the exception that a much larger fraction of the hydroxyl groups are inaccessible to the organochromium reagent. However the disappearance of the sharp band at 3747 cm^{-1} (**Figure 3.6a**) indicates that the isolated OH groups are consumed during the reaction. The difference spectrum **Figure 3.7b** shows that the broad band at ca. 3690 cm^{-1} does not change during the reaction, similar to the case on A_{200}-200. These OH groups are possibly located in the bulk of the silica structure or in small pores and are sterically inaccessible to the Cr(IV) complex (as they were to the $VOCl_3$ reagent used to titrate accessible hydroxyls).[6]

Table 3.3 Quantitative analysis of the products of grafting of $Cr(CH_2C(CH_3)_3)_4$ on S_{952}-200

mass of silica mg	wt.% Cr	μmol Cr	μmol OH[a]	Cr/OH	μmol NpH	NpH/Cr
18.5	1.04	3.7	23.1	0.16	7.3	1.97
23.6	1.19	5.4	29.5	0.18	11.0	2.04
25.4	1.39	6.8	31.8	0.21	12.3	1.81
31.2	1.18	7.1	39.0	0.18	13.9	1.96
20.5	2.31	9.1	25.6	0.36	16.3	1.79
22.8	2.12	9.3	28.5	0.33	17.9	1.92
31.7	1.80	11.0	39.6	0.28	22.0	2.00
						Avg. 1.93±0.07

[a] Calculated based on the number of surface hydroxyl groups on S_{952}-200 (1.25 mmol OH/g silica).[4]

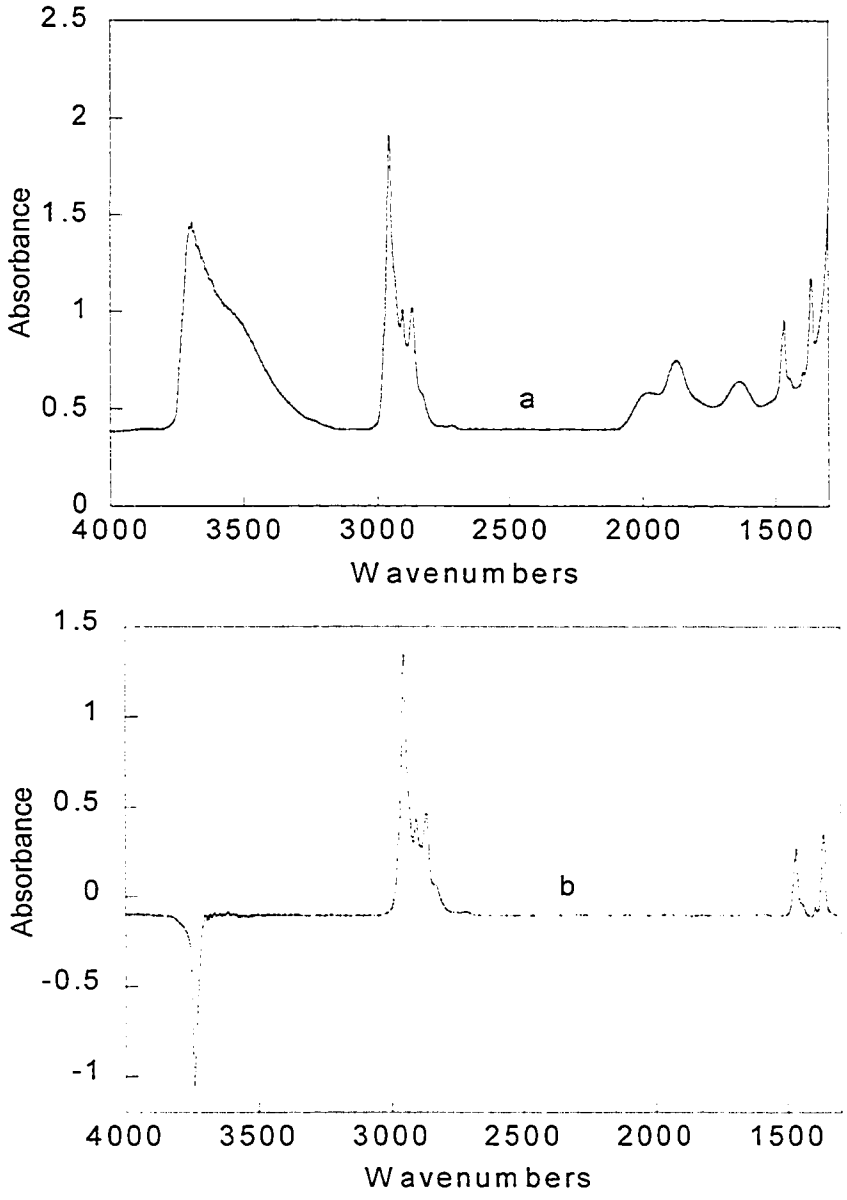

Figure 3.7 FTIR spectra of (a) a self-supporting disk of Sylopol 952 silica, partially dehydroxylated at 200°C, with Cr loading 1.80% after reaction with $Cr(CH_2C(CH_3)_3)_4$; (b) difference spectrum with silica background subtracted.

3.4.3 Thermolysis

3.4.3.1 Stoichiometry

Thermolysis of $(\equiv SiO)_2Cr(CH_2C(CH_3)_3)_2$ on S_{952}-200 was investigated in the same fashion as for A_{200}-200. When $(\equiv SiO)_2Cr(CH_2C(CH_3)_3)_2$ was heated, typically at 71°C, in static vacuum for four hours, neopentane was the exclusive gaseous product, detected by IR and GC. The intensity of IR bands in the ν(CH) stretching region in the spectrum of $(\equiv SiO)_2Cr(CH_2C(CH_3)_3)_2$ decreased by (48±2)%, **Table 3.4**. Furthermore, the yield of neopentane corresponds to (1.1±0.2) per grafted Cr. The reaction therefore occurs with the same precise stoichiometry as shown in equation 3.7 for Aerosil-supported $(\equiv SiO)_2Cr(CH_2C(CH_3)_3)_2$.

3.4.3.2 Kinetics

The kinetics of the thermolysis reaction were investigated *in vacuo* at 73°C in an *in situ* IR cell. To monitor the progress of the surface reaction, the spectrum of the gas phase was recorded at regular time intervals and the ν(CH) region (i.e., the spectrum of product $C(CH_3)_4$) was integrated to give the absorbance values A_t. **Figure 3.8** was thus obtained. The data was fit to the first-order integrated rate equation

Table 3.4 Quantitative analysis of products of thermolysis of $(\equiv SiO)_2Cr(CH_2C(CH_3)_3)_2$ on S_{952}-200

mass silica	Cr	Cr	% loss of surface	NpH	NpH/Cr
mg	wt.%	μmol	ν(CH) [a]	μmol	
23.6	1.19	5.4	48.3	5.4	1.0
25.4	1.39	6.8	46.8	6.1	0.9
22.8	2.12	9.3	50.7	12.2	1.3
29.1	1.66	9.3	47.5	10.2	1.1
			Avg. 48±2		Avg. 1.1±0.2

[a] Based on *in situ* integration of the IR spectrum of the silica pellet in the ν(CH) region, 3200-2800 cm^{-1}, which is proportional to the number of neopentyl ligands present on the surface.

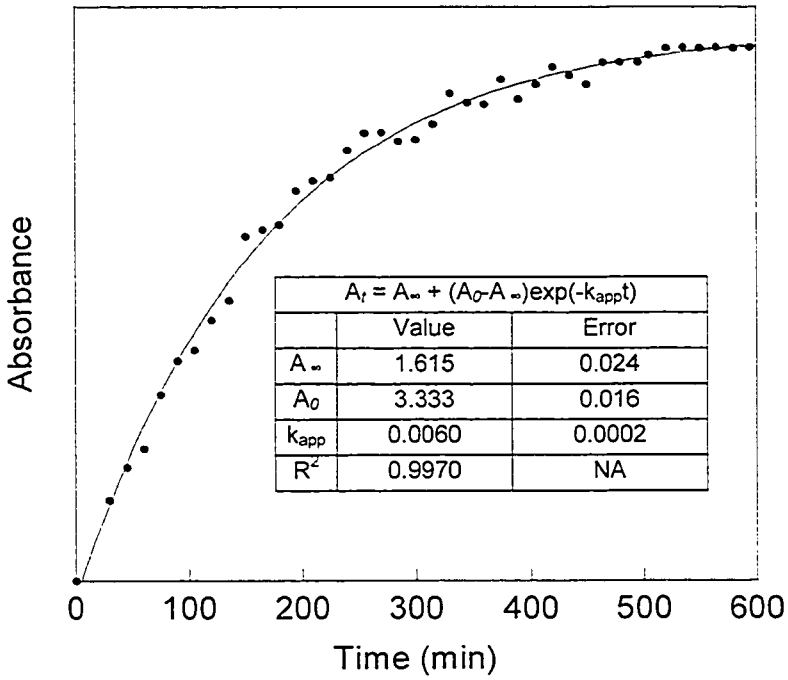

Figure 3.8 Time-resolved evolution of $C(CH_3)_4$ at 73°C from $(\equiv SiO)_2Cr(CH_2C(CH_3)_3)_2$ on a 29.1 mg pellet of S_{952}-200 loaded with 1.66 wt.% Cr.

$A_t = A_0 + (A_\infty - A_0)(e^{-kt})$. The curve fit indicates first-order kinetics with rate constant k(73°C) = (0.0060±0.0002) min^{-1}, intermediate between values measured for materials prepared with Aerosil 200, k(69°C) = (0.0046±0.0002) min^{-1} and k(78°C) = (0.0075±0.0001) min^{-1}. It is also consistent with the temperature dependence shown in the Eyring plot in **Figure 3.4**.

3.4.3.3 Reactivity of Sylopol-supported neopentylidenechromium(IV)

As for A_{200}-200, spectroscopic evidence for the alkylidene nature of the paramagnetic surface complex $(\equiv SiO)_2Cr{=}CHC(CH_3)_3$ on Sylopol 952 is not easy to obtain, since the IR spectrum does not contain a low frequency C-H stretching mode. Therefore the characteristic reaction was again employed. Reaction of $(\equiv SiO)_2Cr{=}CHC(CH_3)_3$ with styrene vapor liberated neohexene, identified by GC, consistent with expected metathesis exchange reaction, equation 3.9. This evidence suggests that the product of thermolysis on S_{952}-200 is $(\equiv SiO)_2Cr{=}CHC(CH_3)_3$.

3.5 Discussion

3.5.1 Thermodynamics of grafting

Grafting of $Cr(CH_2C(CH_3)_3)_4$ onto A_{200}-200 from solution appears to generate the same surface organometallic fragment, $(\equiv SiO)_2Cr(CH_2C(CH_3)_3)_2$, as grafting by

sublimation. This conclusion is based on the results described in section 3.3. We infer that the driving force for grafting includes a significant enthalpic component. On A_{200}-200, the maximum loading of $Cr(CH_2C(CH_3)_3)_4$ obtained by sublimation grafting corresponds to 1.75 wt.% Cr in this research, compared to 1.94 wt.% Cr reported previously.[5] In contrast, the maximum loading obtained by solution grafting was only 0.91 wt.%. Thus, although grafting does occur from solution, only some of the surface hydroxyl groups react with $Cr(CH_2C(CH_3)_3)_4$ under such conditions. Those which react with $Cr(CH_2C(CH_3)_3)_4$ in solution are those for which the driving force is both enthalpic and entropic. For those which do not react under solution conditions, we presume that the enthalpic term is not large enough to make the reaction spontaneous. Heterogeneity of the surface hydroxyls may result in a variation of their pK_a's and, consequently, their reactivity towards organometallic derivatizing agents.

3.5.2 Effect of the nature of the support on grafting chemistry

Both Aerosil 200 and Sylopol 952 are purely siliceous, amorphous materials. However, their morphologies are quite different. The Aerosil is comprised of small (ca. 12 nm), nonporous particles with smooth surfaces while the Sylopol consists of large (ca. 112 μm), porous particles (average pore volume 1.61 mL/g) with considerable surface roughness. Furthermore, the hydroxyl density on each silica after 200°C thermal treatment is quite different: 0.86 mmol/g for Aerosil 200 and 1.25 mmol/g for

Sylopol 952.[7] Nevertheless, the grafting stoichiometry for $Cr(CH_2C(CH_3)_3)_4$ on both types of silica appears to be the same, i.e., reaction with pairs of OH groups to yield the bis(neopentyl)chromium(IV) surface fragment. We conclude that, despite their different morphologies, the local surface chemistry which is important for grafting is similar on Sylopol 952 and Aerosil 200. In both cases, after pretreatment at 200°C, mostly pairs of OH groups react in the manner of equation 3.4.

More hydroxyls are inaccessible for grafting of Sylopol 952 than on Aerosil 200. The roughness of the surface structure of Sylopol, **Scheme 3.2**, may hinder access of the bulky $Cr(CH_2C(CH_3)_3)_4$ molecule to some silanols which are located in smaller pores with narrow entrances. The rugged surface structure of Sylopol 952 was discussed in section 1.4.

Scheme 3.2 Depiction of the rough surface of porous Sylopol silica

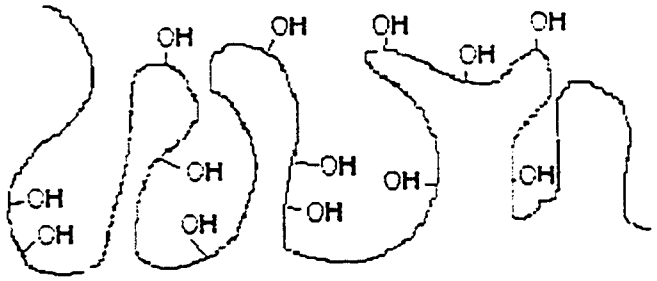

3.5.3 Effect of the nature of the support on thermolysis

Both the stoichiometry (equation 3.7) and rate constant for thermolysis of $(\equiv SiO)_2Cr(CH_2C(CH_3)_3)_2$ are independent of the silica support (Aerosil 200 or Sylopol 952). Recently, Ziegler et al. calculated that α-H abstraction in a bis(ethyl)chromium(IV) model compound is endothermic by 24.6 kcal/mol,[12] equation 3.10.

$$L_2Cr(CH_2CH_3)_2 \rightarrow L_2Cr{=}CHCH_3 + CH_3CH_3 \qquad L = O\text{-}SiH_2\text{-}O\text{-}SiH_2\text{-}O \qquad (3.10)$$

However, there are two reasons to believe that the reaction of the silica-supported analogue is thermodynamically more favorable:

(1) Replacement of the ethyl groups by neopentyl ligands results in substantially more steric crowding, which is relieved upon extrusion of neopentane. Xue et al.[13,14] recently reported quantum mechanical *ab initio* calculations for unimolecular methane elimination from $Ti(CH_3)_4$ and neopentane elimination from $Ti(CH_2C(CH_3)_3)_4$ through α-H abstraction. The calculated reaction energy is 37.5 kcal/mol for methane elimination with an activation energy of 41 kcal/mol. In contrast, the calculated reaction energy for neopentane elimination by α-H abstraction is ca. 27 kcal/mol, with an activation energy of only 18.6 kcal/mol due to relief of steric interactions between neopentyl ligands.

(2) Formation of neopentane gas is entropically favorable. Ziegler et al.[14] estimated that -TΔS contributes -10 kcal/mol to the driving force (ΔG^0) at T=300 K, based on an estimated value of ΔS ~ 36 cal/mol.K.

From these arguments we conclude that it is reasonable to expect mild heating to induce α-H abstraction in silica-supported bis(neopentyl)chromium.

Børve et al. considered a model which provides a more authentic representation of the chromium-silica interaction.[15] They constructed silica "ligands" with different ring sizes, **Figure 3.9**. As the ring size increases, the angle ∠OCrO increases, and the angle ∠CCrC of the coordinated CrR_2 fragment gets correspondingly smaller. The effect is to increase steric crowding and decrease the barrier for α-H abstraction. In the case of R = methyl, $\Delta H^{\ddagger}$ for α-H transfer was calculated to be too high to generate methylidenechromium(IV) at 60-80°C. However, the barrier for R = neopentyl (not calculated) is certain to be lower, for the same reasons described above.

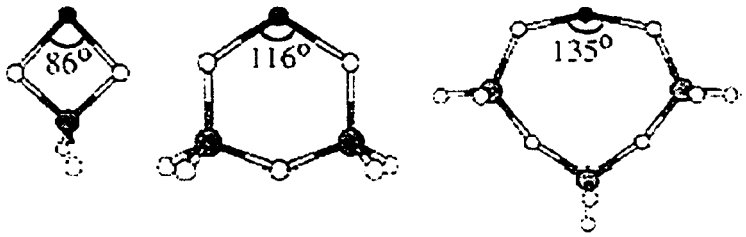

Figure 3.9 Børve's cluster models for Cr on the silica surface: n_{Si} = 1 (left), n_{Si} = 2 (middle), and n_{Si} = 3 (right). The elements are coded on a gray scale according to H(white) < O < Si < Cr (dark gray).[15]

In previous work,[16] it was suggested that a neighboring siloxane may assist α-H abstraction, **Scheme 3.3**. Coordination of oxygen atoms from nearby siloxane bridges to Cr further increases steric strain in the reactant as well as stabilizes the neopentylidene product, thereby assisting α-H abstraction. Børve et al. calculated the effect of coordinating a water molecule to a cluster model containing the bis(methyl)chromium(IV) fragment. The product methylidenechromium(IV) cluster was stabilized by 12.4 kcal/mol through a favorable interaction with the water ligand, although no bound state for the bis(methyl)chromium complex was found. This suggests that similar interactions are plausible on the silica surface; however, the Cr-siloxane interaction may be important only after the transition state for α-H elimination. This is consistent with the lack of an effect of the silica support (Aerosil vs. Sylopol) on the rate constant for neopentylidene formation, even though siloxane-Cr interactions are expected to be considerably different on the two surfaces.

Scheme 3.3 Siloxane-assisted α-H abstraction on the surface

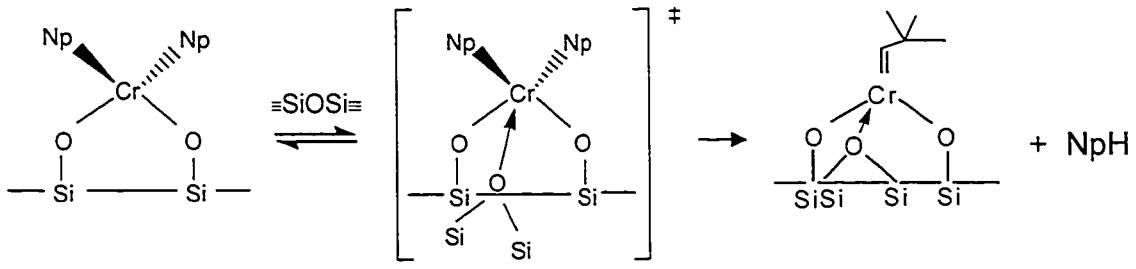

3.6 Conclusion

Well-defined surface organometallic fragments $(\equiv SiO)_2CrR_2$ ($R=CH_2C(CH_3)_3$, **1a**, or $CH_2Si(CH_3)_3$, **1b**) were obtained by sublimation grafting onto A_{200}-200. First order thermal transformation of $(\equiv SiO)_2Cr(CH_2C(CH_3)_3)_2$ generated $(\equiv SiO)_2Cr{=}CHC(CH_3)_3$ by intramolecular α-H abstraction, as previously reported. A solution grafting technique was also shown to be practical. On S_{952}-200, the grafting and thermolysis reactions were undertaken in the same fashion as for A_{200}-200. The subsequent metathetical exchange of $(\equiv SiO)_2Cr{=}CHC(CH_3)_3$ with styrene is consistent with its previously reported reactivity on A_{200}-200. The nature of the silica support therefore does not appear to substantially influence either the grafting reaction or neopentylidene formation. However, evidence for an effect of the support on the reactivity of surface complexes was found in their olefin polymerization reactions, described in the following chapter.

3.7 References

(1) Carrick, W. L.; Chasar, A. G.; Smith, J. J. *J. Am. Chem. Soc.* **1960**, *82*, 5319.

(2) Quignard, F.; Lecuyer, C.; Bougault, C.; Lefebvre, F.; Choplin, A.; Olivier, D.; Basset, J.-M. *Inorg. Chem.* **1992**, *31*, 928.

(3) Schwartz, J.; Ward, M. D. *J. Mol. Catal.* **1980**, *8*, 465.

(4) Taha, Z. A.; Scott, S. L. manuscript in preparation.

(5) Amor Nait Ajjou, J.; Scott, S. L. *Organometallics* **1997**, *16*, 86-92.

(6) Rice, G. L.; Scott, S. L. *Langmuir* **1997**, *13*, 1545-1551.

(7) Morrow, B. A. *Stud. Surf. Sci. Catal.* **1990**, *57A*, 161-224

(8) Colthrup, N. B.; Daly, L. H.; Wilberley, S. E. *Introduction to Infrared and Raman Spectroscopy;* Academic: New York, 1964.

(9) Kruse, W. *J. Organomet. Chem.* **1972**, *42*, C39-C42.

(10) Amor Nait Ajjou, J.; Scott, S. L. *J. Am. Chem. Soc.* **1998**, *120*, 13436-13443.

(11) Avnir, D.; Farin, D. *Nature* **1984**, *308*, 261.

(12) Schmid, R., Ziegler, T. *Can. J. Chem.* **2000**, *78*, 265-269

(13) Wu, Y. D.; Peng, Z. H.; Xue, Z. L. *J. Am. Chem. Soc.* **1996**, *118*, 9772-9777.

(14) Wu, Y. D.; Peng, Z. H.; Chan, K. W. K.; Liu, X. Z.; Tuinman, A. A.; Xue, Z. L. *Organometallics* **1999**, *18*, 2081-2090.

(15) Espelid, Ø., Børve, K. J. *J. Catal.* **2000**, *195,* 125-139.

(16) Amor Nait Ajjou, J. Ph.D. thesis, University of Ottawa, 2000.

Chapter 4

Olefin Polymerization Catalyzed by Silica-Supported Chromium Complexes

4.1 Introduction

The Phillips catalyst, CrO_3/SiO_2, is active for olefin polymerization even without an alkylaluminum activator.[1] However, the number of active sites on the Phillips catalyst is reported to range from only 0.01 up to ca. 10%, where the fraction of active sites depends on the chromium loading,[2] the ethylene pressure,[3] and the method used for active site counting.[4,5] Consequently, little is known about the structure of the active site or how polymerization is initiated. Previous research in the Scott group demonstrated that a silica-supported organochromium(IV) complex, $(\equiv SiO)_2Cr{=}CHC(CH_3)_3$, initiates the polymerization of various olefins without an activator.[6] However, for the Aerosil 200-supported catalyst, it was estimated that only 20-30% of the Cr sites are activated at low ethylene pressures (50-250 Torr), despite their apparent uniformity.

Empirical evidence for the formulation of the alkylidene complexes as $(\equiv SiO)_2Cr{=}CHC(CH_3)_3$[7] does not take into account that the coordination number of the metal is unlikely to remain three in the presence of many possible oxygen donor atoms

disposed in proximity around the supported organometallic fragment. Association with the oxygen of a nearby siloxane bridge to form a pseudo-tetrahedral surface complex is a strong possibility, equation 4.1.

$$(\equiv SiO)_2Cr{=}CHC(CH_3)_3 + \equiv SiOSi\equiv \rightarrow (\equiv SiO)_2(\equiv Si_2O)Cr{=}CHC(CH_3)_3 \qquad (4.1)$$

Siloxane coordination of surface Cr sites was suggested to be responsible for the observed pressure-dependence of the fraction of active sites,[6] provided ethylene must displace the siloxane before reacting at the alkylidene site.

Direct probing of siloxane-Cr interactions is difficult due to the lack of characteristic spectroscopic evidence. However, the siloxane disposition might be expected to be substantially different if the structure of the underlying silica were changed. Previous work used Aerosil silica, a nonporous material with a flat surface that is often used to construct catalyst models. Sylopol 952 is an alternative silica widely used in industrial catalysts. As described in the previous chapter, this silica is a porous gel with a rough internal surface. The surface roughness of Sylopol 952 may contribute a larger number of siloxanes in close proximity to the active sites. One objective of this research was to probe the effect of varying the silica support on the polymerization activity.

During this investigation, we unexpectedly encountered evidence about the nature of the propagation sites. Although $(\equiv SiO)_2Cr{=}CHC(CH_3)_3$ is known to initiate

ethylene polymerization, the propagation mechanism does not appear to involve alkylidene intermediates.[6] The nature of the transformation of the initiating site into a propagating site became a second objective of this investigation, especially since prior experimental[8] and subsequent theoretical[9,10] studies showed that bis(alkyl)chromium(IV) sites cannot readily initiate polymerization.

Polyethylene is a hydrocarbon homopolymer with no stereochemistry. Homopolymers of other α-olefins have a variety of structures depending on their stereochemistry. Different structures possess different properties and hence are suited for different applications. Polypropylene has three stereoisomers, **Figure 4.1**. The interest in stereospecific polymerization and the observation that $(\equiv SiO)_2Cr{=}CHC(CH_3)_3$ generates moderately isotactic polypropylene[8] led us to further investigate the Cr-catalyzed homopolymerization of propylene, especially its kinetics. In previous research, it was found that $(\equiv SiO)_2Cr{=}CHC(CH_3)_3$ initiates the homopolymerization of 1-hexene. Furthermore, various ethylene oligomers (1-butene, 1-hexene, etc.) are created during homopolymerization of ethylene, and may be incorporated into the growing polyethylene chains to create copolymers.[8]

The extent of copolymerization depends on the reactivity ratio of the active site for each monomer pair. In this chapter, the rate of propylene homopolymerization over a Cr/SiO_2 catalyst is reported and compared to rates for ethylene and 1-hexene.

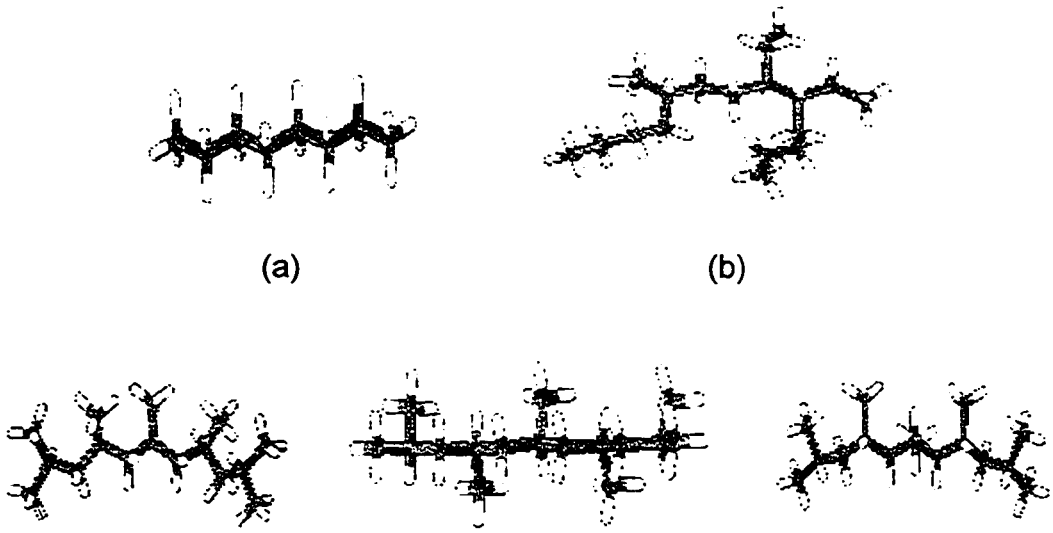

Figure 4.1 3D stick representations of (a) linear polyethylene; (b) branched polyethylene; (c) isotactic polypropylene; (d) syndiotactic polypropylene; (e) atactic polypropylene. The hydrogens are shown in white and the carbons in green.

4.2 Ethylene polymerization on Aerosil 200-supported catalysts

4.2.1 Polymerization initiated by $(\equiv SiO)_2Cr{=}CHC(CH_3)_3$

In the previous chapter, the surface complex $(\equiv SiO)_2Cr(CH_2C(CH_3)_3)_2$ supported on Aerosil silica was demonstrated to undergo thermolysis in vacuum at ca. 70°C to produce a well-defined chemisorbed surface organometallic fragment characterized as $(\equiv SiO)_2Cr{=}CHC(CH_3)_3$. When the unthermolyzed silica-supported bis(neopentyl)-chromium(IV) complex was exposed to 65 Torr ethylene at room temperature, no polymerization was detected. (Henceforth, in this research "low pressure of ethylene" refers to $P_{C2H4} < 100$ Torr). However, after they were heated together to 70°C for an hour and a half, the silica pellet was observed to have undergone a color change from its original orange color to white, and a plastic coating had formed on its surface. Meanwhile, the pellet had thickened and become rigid. These observations are consistent with polymerization of ethylene, and further suggest that only the neopentylidene form, $(\equiv SiO)_2Cr{=}CHC(CH_3)_3$, and not the bis(neopentyl) form, $(\equiv SiO)_2Cr(CH_2C(CH_3)_3)_2$, can initiate polymerization at low pressures of ethylene.

A further experiment supported this assertion. $(\equiv SiO)_2Cr{=}CHC(CH_3)_3$ was prepared independently by thermolysis of $(\equiv SiO)_2Cr(CH_2C(CH_3)_3)_2$, then exposed to 58 Torr ethylene at room temperature. Within one hour, polyethylene was visible

to the naked eye as well as by *in situ* IR. $(\equiv SiO)_2Cr{=}CHC(CH_3)_3$-initiated ethylene polymerization is described in equation 4.2:

$$(\equiv SiO)_2Cr{=}CHC(CH_3)_3 \xrightarrow{n\ CH_2{=}CH_2} \text{polyethylene} \qquad (4.2)$$

These results confirm previous research in the Scott group in terms of the reactivity of silica-supported organochromium(IV) species towards low pressures of ethylene.[8]

Although we did not test the reactivity of $(\equiv SiO)_2Cr{=}CHC(CH_3)_3$ supported on Aerosil 200 towards ethylene at higher pressures, we are confident that it retains its reactivity under these conditions. This assertion is based on an earlier investigation of the polymerization kinetics, which demonstrated that the order of the reaction is one with respect to pressure of ethylene.[6]

4.2.1.1 IR characterization

Gas phase polymerization is characterized by a significant increase in intensity in the ν(C-H) region of the *in situ* IR spectrum of the modified silica surface, **Figure 4.2 (I)**. The increase in intensity at 1471 cm^{-1}, **Figure 4.2(II)**, is attributed to the methylene bending mode of polyethylene. This band is characteristic of the crystalline phase of linear polyethylene.[11,12,13,14] In the spectral "window" region on silica between 850 and 700 cm^{-1}, two new bands at 730 and 718 cm^{-1} were observed, **Figure 4.2(III)**, and are

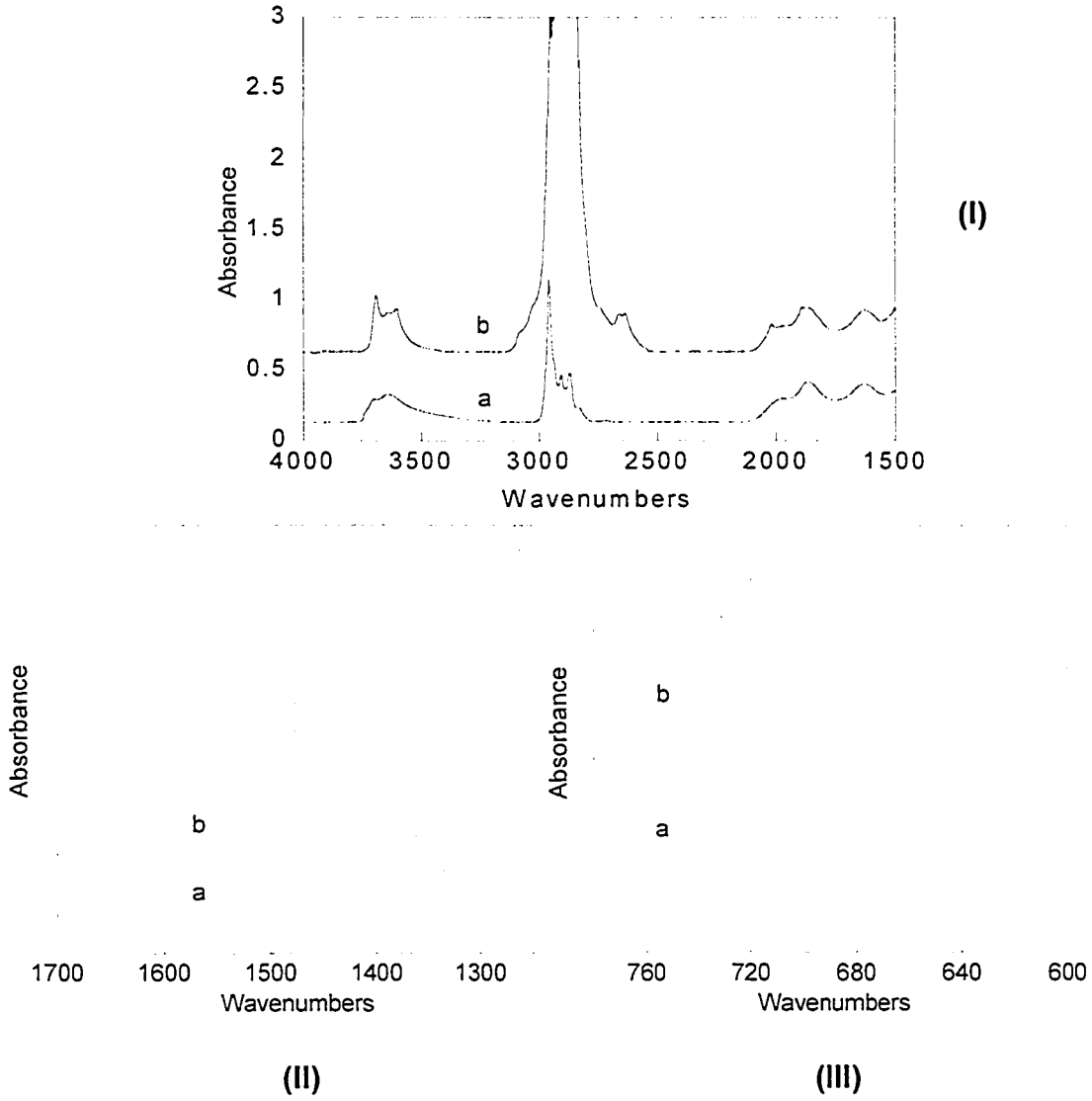

Figure 4.2 *In situ* IR spectra of (a) an Aerosil silica surface modified by $(\equiv SiO)_2Cr{=}CHC(CH_3)_3$; (b) after reaction with 58 Torr ethylene, followed by evacuation of volatiles.

assigned to the methylene rocking mode. In crystalline polyethylene, a splitting of this mode is always observed. Consequently, measurement of the relative intensities of the bands at 718 and 730 cm^{-1} can be used to estimate the relative crystallinity of the polyethylene. For our polymer, the extent of relative crystallinity is estimated to be 80%.[15]

4.2.1.2 Kinetics

The kinetics of ethylene polymerization were examined with 65 Torr $CH_2=CH_2$ on a 19.8 mg Aerosil 200 pellet with 1.68 wt.% Cr loading as $(\equiv SiO)_2Cr(CH_2C(CH_3)_3)_2$. As described above, there is no reaction at room temperature. The reactor was heated so that the temperature climbed slowly, reaching 70°C after 65 minutes. The onset of ethylene consumption was noted at 50 minutes. Ethylene uptake was monitored by following absorbance changes in the ν(C-H) region of the gas phase IR spectrum, **Figure 4.3**. The curve fit to the data after the activation temperature (70°C) was achieved demonstrates that the reaction is pseudo-first-order, with $k_{app}=(0.072\pm0.005)$ min^{-1}. Since the value of k_{app} was previously shown to be proportional to the amount of Cr present,[6] this corresponds to a second-order rate constant $k(70°C)=(190\pm3)$ $s^{-1}(mol\ Cr)^{-1}$. For comparison, the previously reported value is $k=(1210\pm3)$ $s^{-1}(mol\ Cr)^{-1}$ for ethylene polymerization initiated by pre-formed $(\equiv SiO)_2Cr{=}CHC(CH_3)_3$ at 70°C.[6] This

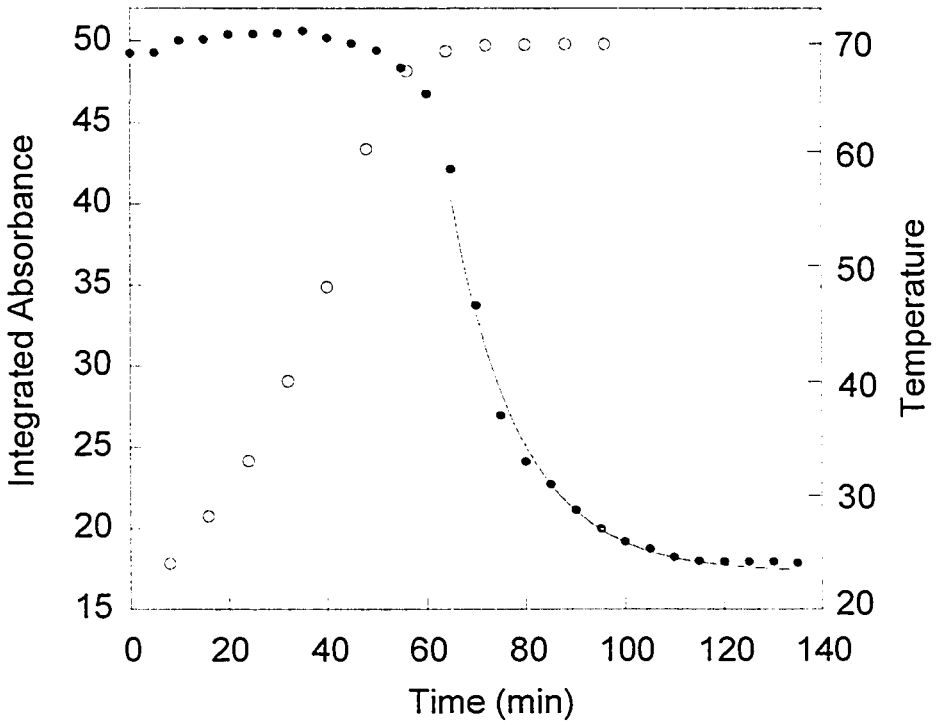

$A_t = A_\infty + (A_0 - A_\infty)\exp(-k_{app}t)$		
	Value	Error
A_∞	17.0	0.4
A_0	2527	887
k_{app}	0.072	0.005
R^2	0.9946	NA

Figure 4.3 Time-resolved consumption of ethylene (65 Torr) during polymerization by $(\equiv SiO)_2Cr{=}CHC(CH_3)_3$ produced *in situ* by heating $(\equiv SiO)_2Cr(CH_2C(CH_3)_3)_2$ on A_{200}-200 (solid circles). The temperature profile is shown by the open circles.

difference will be discussed in following section. This experiment demonstrates that the initiating site is $(\equiv SiO)_2Cr{=}CHC(CH_3)_3$, formed *in situ* by thermolysis at 70°C of $(\equiv SiO)_2Cr(CH_2C(CH_3)_3)_2$ when the pressure of ethylene is low.

4.2.2 Polymerization initiated by $(\equiv SiO)_2Cr(CH_2C(CH_3)_3)_2$

As shown above, $(\equiv SiO)_2Cr(CH_2C(CH_3)_3)_2$ is incapable of initiating ethylene polymerization at room temperature and low pressures (ca. 100 Torr). Reaction with a slightly higher ethylene pressure, 238 Torr, was also attempted, but no polyethylene was detected. When the ethylene pressure was increased to 400 Torr, there was still no polymer formed on the surface. However, when the ethylene pressure reached 520 Torr, polymerization occurred at room temperature without heating. (Henceforth, in this research, "high pressure of ethylene" refers to 400 Torr < P_{C2H4} < 760 Torr). Thus, when a 28.6 mg self-supporting disk of A_{200}-200 silica modified with $(\equiv SiO)_2Cr(CH_2C(CH_3)_3)_2$ (1.29 wt.% Cr) was exposed to this pressure of purified ethylene at room temperature, polyethylene was observed on the surface after 15 minutes. The orange color of the silica became paler, then white, and the initially thin, fragile silica pellet became a thick, rigid disk, confirming the formation of a hard polymer film.

4.2.2.1 IR characterization

The surface was characterized by *in situ* IR spectroscopy, **Figure 4.4**. New bands in the ν(C-H) region at 2924 and 2850 cm^{-1} are due to the asymmetric and symmetric CH_2 stretching modes of polyethylene. The methylene bending mode was observed at 1471 cm^{-1}, confirming the presence of the crystalline phase of linear polyethylene. The IR spectrum also shows bands at 1377 and 908 cm^{-1}, due to vibrations of methyl and vinyl end groups, respectively, of the polymer chains, **Figure 4.4c**.

4.2.2.2 GC Analysis of volatiles

Volatile products present after polymerization were identified by GC based on the retention times for pure standards. In addition to neopentane, the following olefins were identified: 1-hexene, neohexene and 4,4-dimethyl-1-pentene, **Figure 4.5**. The observation of neohexene is particularly noteworthy (see Discussion). For comparison, the volatiles during ethylene polymerization over $(\equiv SiO)_2Cr{=}CHC(CH_3)_3$ on A_{200}-200 in a previous investigation by the Scott group included 4,4-dimethyl-1-pentene and even-numbered carbon olefins such as butene, hexene, octene and decene isomers, etc., but no neohexene.

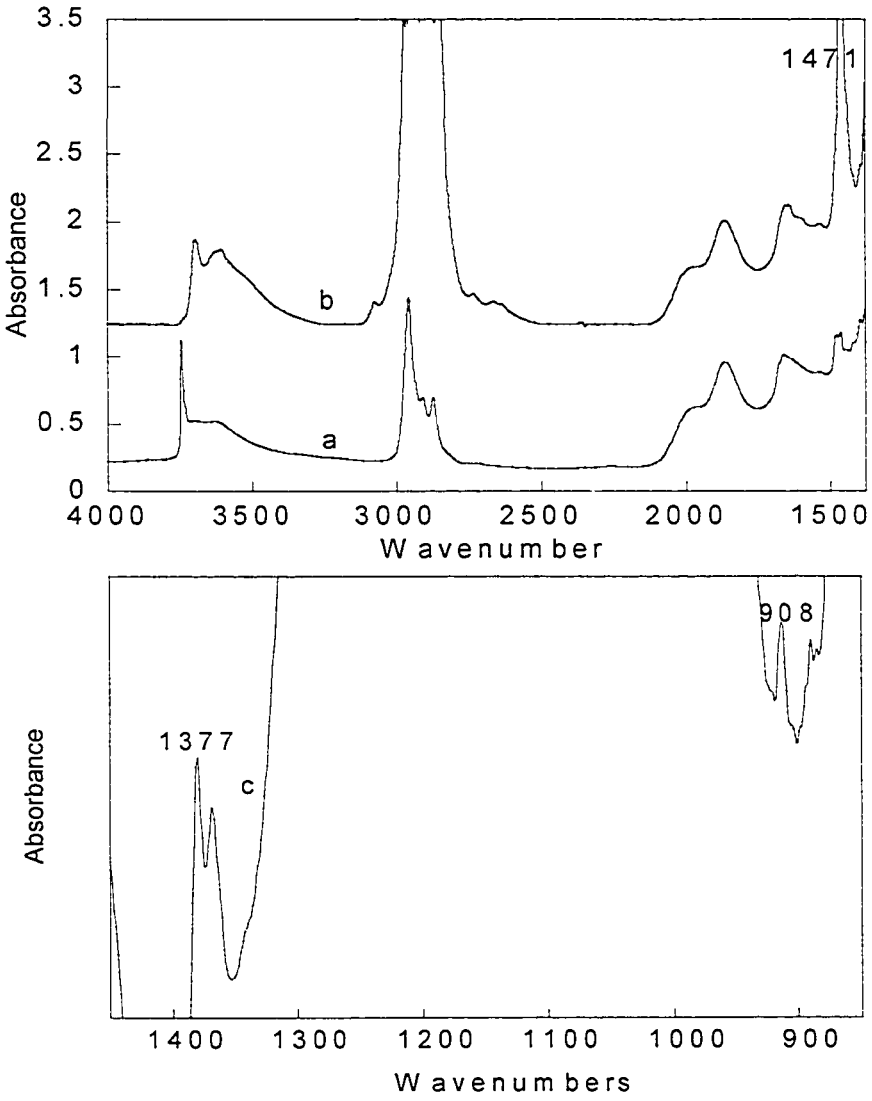

Figure 4.4 IR spectra of (a) $(\equiv SiO)_2Cr(CH_2C(CH_3)_3)_2$; and (b, c) after addition of 520 Torr ethylene, followed by evacuation of volatiles, on a 28.6 mg Aerosil 200 silica loaded with 1.29 wt.% Cr.

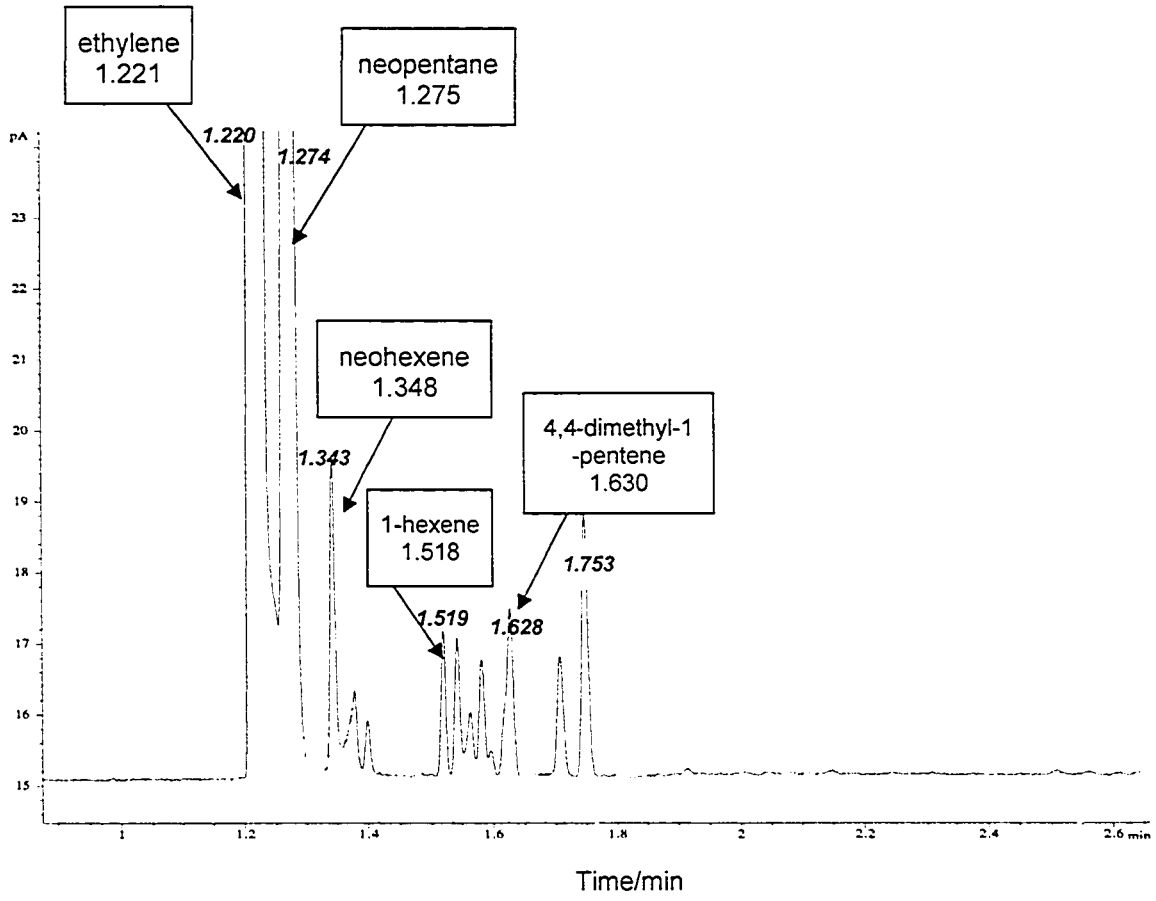

Figure 4.5 Gas chromatogram of volatile products produced during polymerization of 520 Torr C_2H_4 over $(\equiv SiO)_2Cr(CH_2C(CH_3)_3)_2$ on A_{200}-200. The boxes indicate the retention times of standards.

4.3 Ethylene polymerization on Sylopol 952 silica-supported catalysts

Upon grafting $Cr(CH_2C(CH_3)_3)_4$ onto a 22.8 mg pellet of Sylopol 952, $(\equiv SiO)_2Cr(CH_2C(CH_3)_3)_2$ was obtained at 2.21 wt.% Cr loading. Then, 70 Torr ethylene was introduced into the *in situ* IR cell. As expected, polymerization is not spontaneous at such a low pressure, as was observed for $(\equiv SiO)_2Cr(CH_2C(CH_3)_3)_2$ on A_{200}-200. Neither was polyethylene detected upon addition of 400 Torr ethylene.

4.3.1 Polymerization initiated by $(\equiv SiO)_2Cr{=}CHC(CH_3)_3$

Due to the similarity of grafting and thermolysis chemistry on Sylopol and Aerosil silicas, the Sylopol surface fragment $(\equiv SiO)_2Cr{=}CHC(CH_3)_3$ was expected to be capable of initiating ethylene polymerization at low pressure. Therefore, it came as a surprise that, under the same experimental conditions as for the Aerosil silica-supported catalyst, $(\equiv SiO)_2Cr{=}CHC(CH_3)_3$ on S_{952}-200 is inert towards 70 Torr ethylene at room temperature. Increasing the temperature to 76°C, a temperature at which $(\equiv SiO)_2Cr{=}CHC(CH_3)_3$ is stable, also failed to initiate polymerization. The Cr-modified silica retained its original orange color during the above treatment, confirming the absence of decomposition. Furthermore, the gas phase IR spectrum showed no uptake of ethylene, **Figure 4.6**. Only a slight increase of absorbance in the ν(CH)

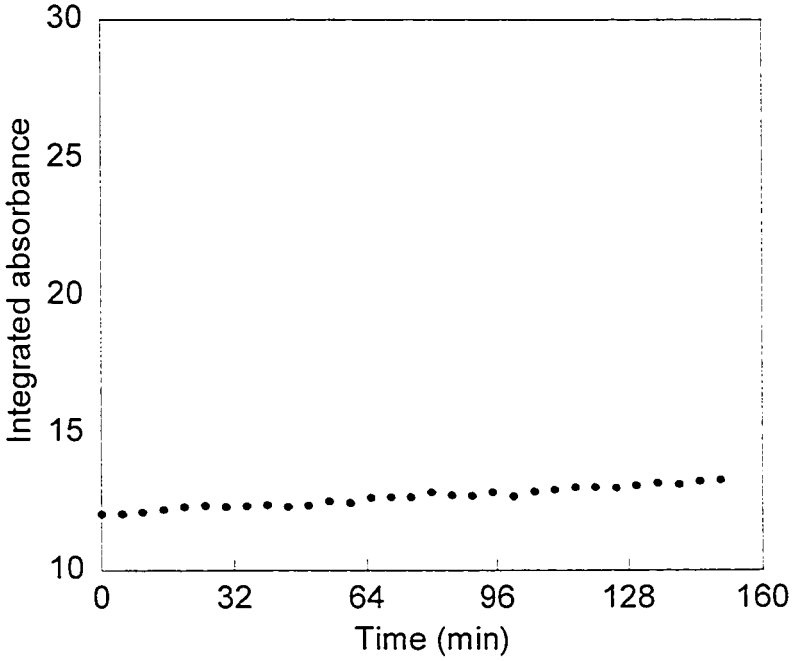

Figure 4.6 Integrated absorbance in the ν(CH) region of the IR spectrum of the gas phase above $(\equiv SiO)_2Cr=CHC(CH_3)_3$ on S_{952}-200 in the presence of 70 Torr ethylene, as a function of time at 76°C.

region of the gas phase IR spectrum was observed, possibly due to a small amount of thermolysis of residual $(\equiv SiO)_2Cr(CH_2C(CH_3)_3)_2$ at 76°C resulting in the liberation of neopentane into the gas phase. Failure to obtain polyethylene in this way on Sylopol silica was reproduced in three independent experiments with Cr loadings from 1.39-2.21 wt.%, and ethylene pressures of ca. 100 Torr. A further trial with 400 Torr ethylene also failed to produce polyethylene. However, when the pressure was increased to 610 Torr, the silica pellet became rigid within 30 minutes as a white plastic disk formed on its surface.

4.3.1.1 IR characterization

In the experiment described above, an *in situ* IR spectrum of the surface showed a dramatic increase in intensity in the ν(CH) and $\delta(CH_2)$ regions, characteristic of the formation of polyethylene, **Figure 4.7**. Two new bands at 730 and 718 cm^{-1} are assigned to the methylene rocking mode of crystalline polyethylene. For this polyethylene, the relative crystallinity is 59%.[15]

4.3.1.2 GC analysis of volatiles

The gas phase remaining after polymerization was analyzed by GC. Based on retention times of standards, compounds identified in the mixture of the volatiles

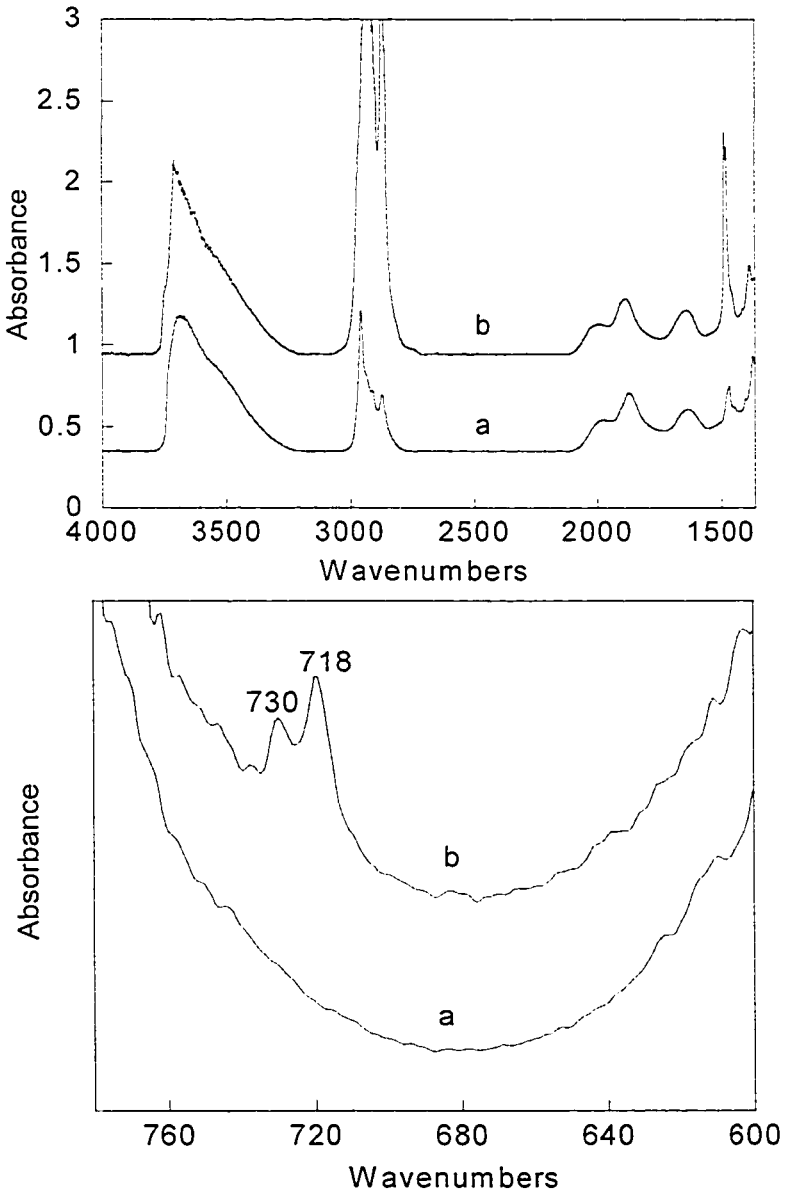

Figure 4.7 IR spectra of (a) a Sylopol silica surface modified by $(\equiv SiO)_2Cr{=}CHC(CH_3)_3$; and (b) after addition of 610 Torr ethylene, followed by evacuation of volatiles.

include: (1) neopentane (partially overlapped with ethylene); (2) 1-hexene; (3) neohexene; and (4) 4,4-dimethyl-1-pentene, **Figure 4.8**. These are the same volatiles as were observed during ethylene polymerization initiated by $(\equiv SiO)_2Cr(CH_2C(CH_3)_3)_2$ on A_{200}-200, and may indicate that the initiation mechanism is the same for both catalysts.

4.3.2 Polymerization initiated by $(\equiv SiO)_2Cr(CH_2C(CH_3)_3)_2$

It was reported in section 4.3 that polymerization was not spontaneously initiated by $(\equiv SiO)_2Cr(CH_2C(CH_3)_3)_2$ supported on S_{952}-200 at low pressures of ethylene ($\leq$ 400 Torr). Nevertheless, the observed initiation of ethylene polymerization by $(\equiv SiO)_2Cr(CH_2C(CH_3)_3)_2$ on A_{200}-200 in the presence of higher pressures of ethylene led us to investigate the reactivity of $(\equiv SiO)_2Cr(CH_2C(CH_3)_3)_2$ supported on S_{952}-200 towards higher pressures of ethylene.

In the presence of 580 Torr ethylene, the orange Cr-modified silica pellet turned white, and a polymer film was visible on the surface within half an hour. A second independent experiment was undertaken with 640 Torr ethylene and also resulted in polymerization.

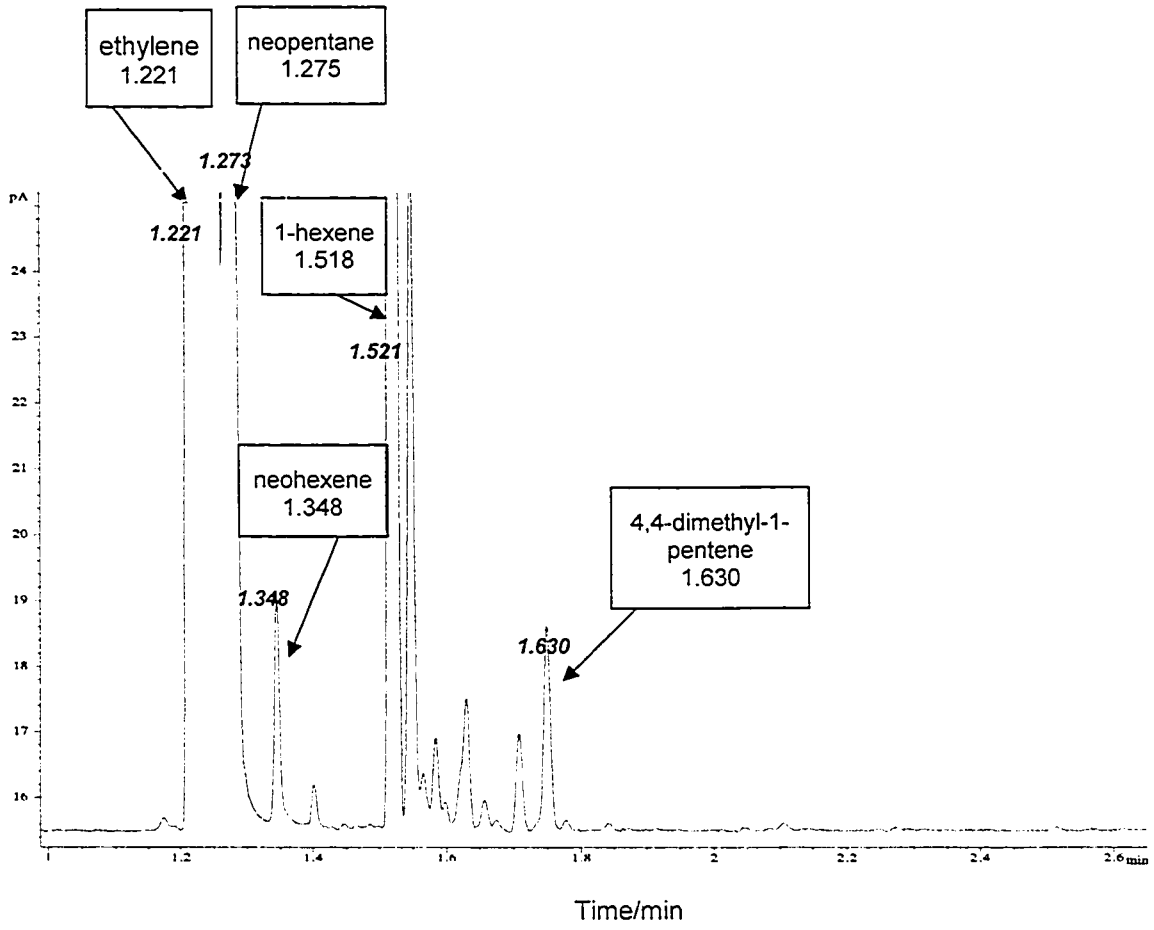

Figure 4.8 Gas chromatogram of volatile products produced during polymerization of 610 Torr C_2H_4 initiated by $(\equiv SiO)_2Cr{=}CHC(CH_3)_3$ supported on S_{952}-200. The boxes indicate retention times of standards.

4.3.2.1 IR characterization

After evacuation of unreacted ethylene, the IR spectrum of the silica pellet showed an increase in intensity in the ν(CH) region, and the methylene bending mode at 1471 cm^{-1} along with two new bands for the methylene rocking mode at 718 and 730 cm^{-1}, **Figure 4.9**. These observations confirm the presence of polyethylene.

4.3.2.2 GC analysis of volatiles

Gas phase products from the ethylene polymerization initiated by $(\equiv SiO)_2Cr(CH_2C(CH_3)_3)_2$ supported on S_{952}-200 were detected by GC and identified as neopentane, 1-hexene, neohexene and 4,4-dimethyl-1-pentene, by comparison to the retention times of the respective pure compounds, **Figure 4.10**. The similarity of this result to that of $(\equiv SiO)_2Cr(CH_2C(CH_3)_3)_2$ supported on A_{200}-200 suggests that in the presence of high pressures of ethylene, the mechanism of initiation of polymerization may be the same regardless of the silica support.

4.4 Propylene polymerization

When $(\equiv SiO)_2Cr{=}CHC(CH_3)_3$ supported on A_{200}-200 was exposed to 80 Torr propylene at room temperature, physical changes were observed after 15 minutes. The

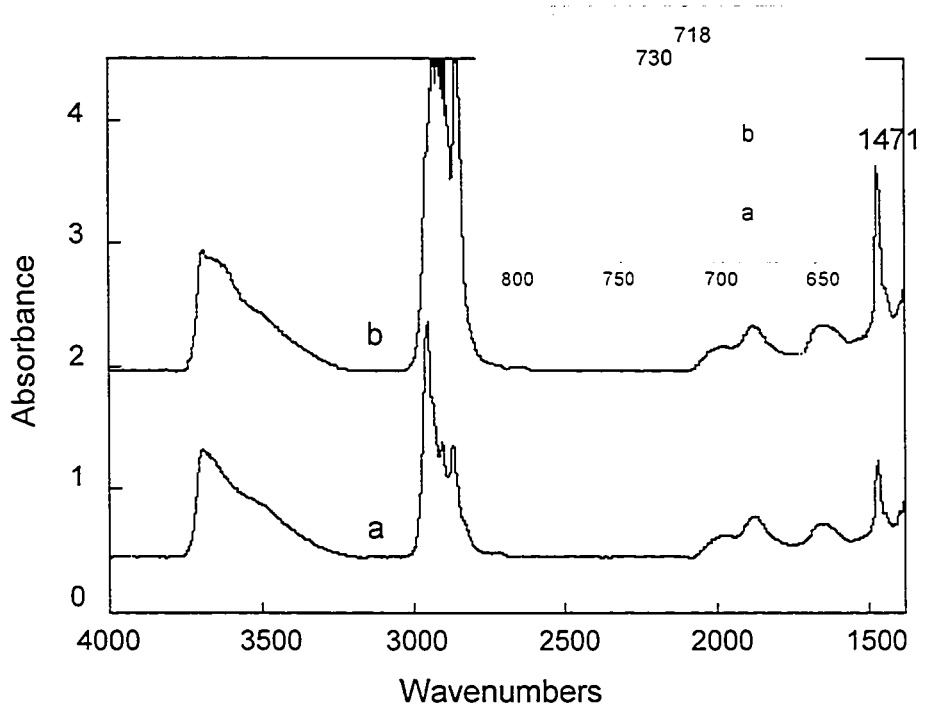

Figure 4.9 IR spectra of (a) $(\equiv SiO)_2Cr(CH_2C(CH_3)_3)_2$ supported on S_{952}-200; and (b) after addition of 580 Torr ethylene, followed by evacuation of volatiles.

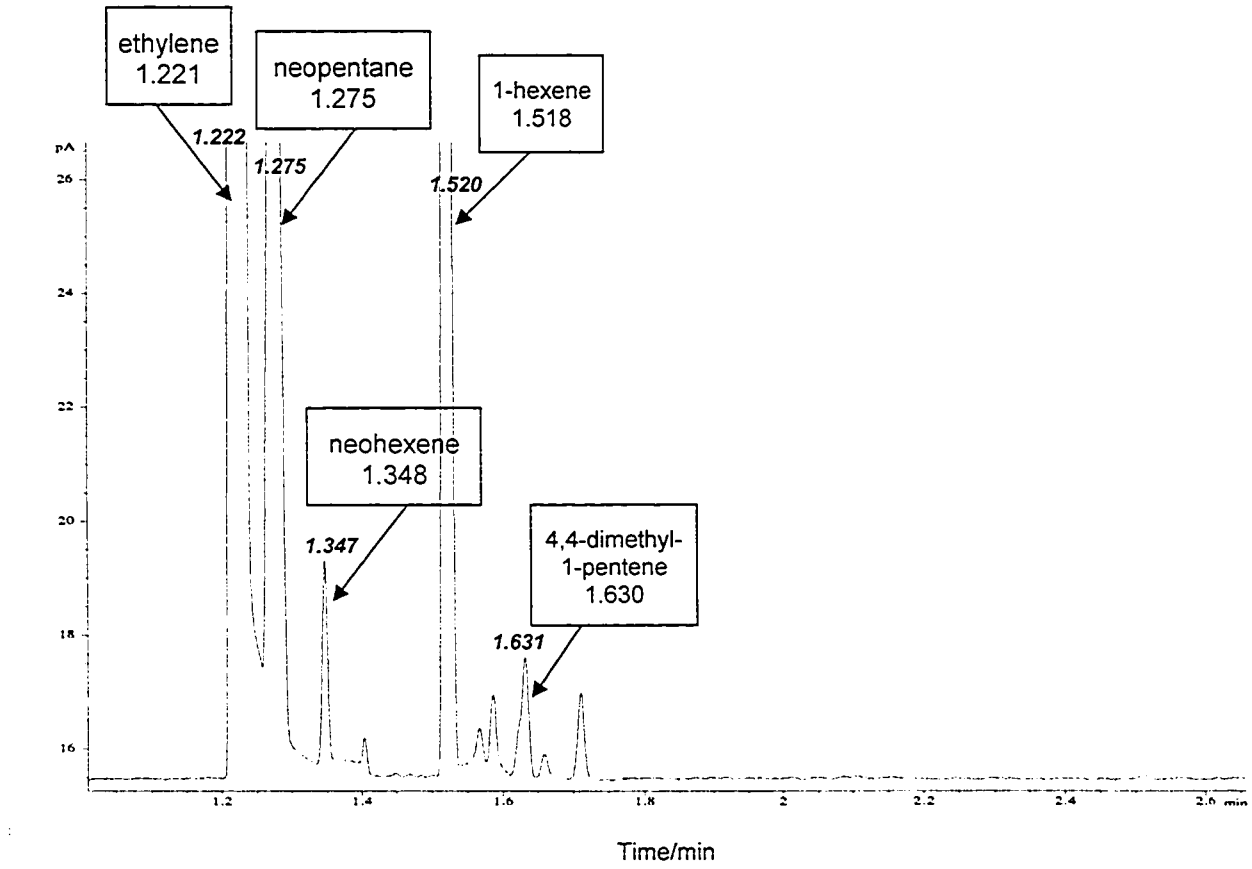

Figure 4.10 Gas chromatogram of volatile products produced during polymerization of 580 Torr C_2H_4 initiated by $(\equiv SiO)_2Cr(CH_2C(CH_3)_3)_2$ on S_{952}-200. Boxes indicate retention times of pure compounds.

Cr-modified pellet changed color from orange to white and from transparent to opaque.

4.4.1 IR characterization

In the ν(CH) region of the *in situ* IR spectrum, new bands at 2958, 2921, 2873 and 2841 cm^{-1} are assigned to the asymmetric and symmetric CH_3 and CH_2 stretching modes of polypropylene, **Figure 4.11**. In the low frequency region, peaks at 1461 and 1377 cm^{-1} are the corresponding methyl and methylene deformation modes. Comparison of spectra recorded after 1.5 hours and 50 hours addition of propylene shows that the polymerization is very slow.

4.4.2 Kinetics

The kinetics of the reaction between propylene and $(\equiv SiO)_2Cr{=}CHC(CH_3)_3$ were investigated on a 45.4 mg Aerosil 200 silica pellet containing 0.726 mg Cr. At 22.2°C, 80 Torr propylene was introduced into the *in situ* IR cell and the gas phase IR spectrum was recorded at regular time intervals. By integration of the IR intensity in the ν(CH) region, we inferred the progress of the polymerization reaction occurring on the surface. The data was fit to a single exponential function, **Figure 4.12a**, and indicated a pseudo-first-order reaction with an apparent rate constant $k_{app}(22.2°C)$ = (0.0026±0.0001) min^{-1}. Two other independent kinetics experiments were carried out

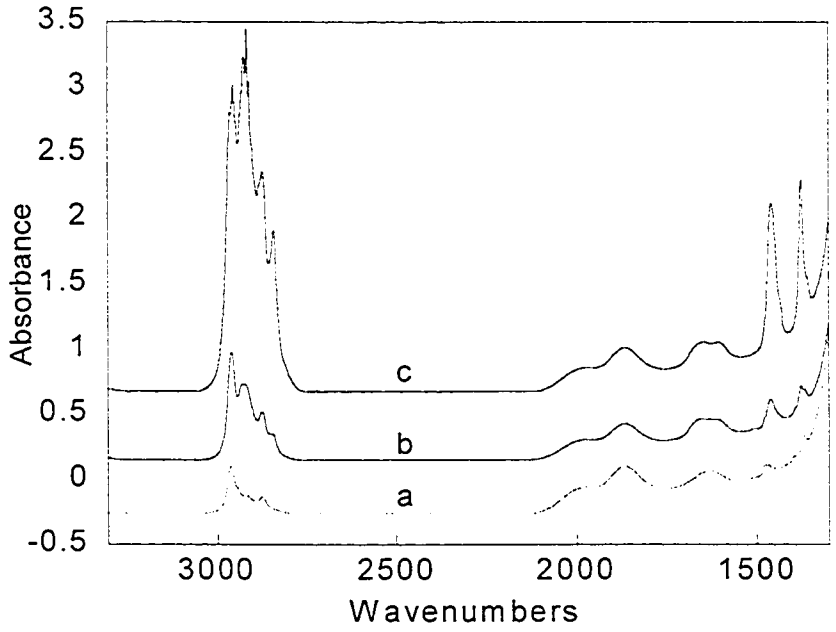

Figure 4.11 IR spectra of (a) $(\equiv SiO)_2Cr{=}CHC(CH_3)_3$; (b) 1.5 hours after addition of 80 Torr propylene; and (c) 50 hours after addition of 80 Torr propylene.

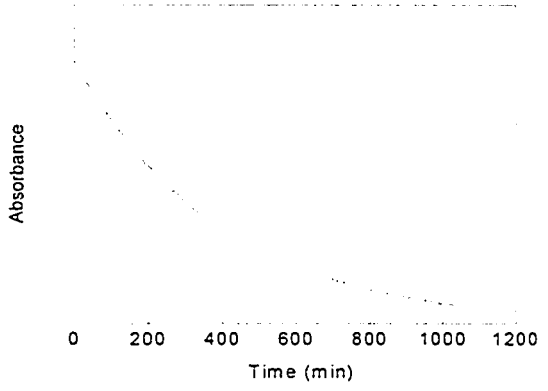

a

$A = A_\infty + (A_0 - A_\infty)\exp(-k_{app}t)$		
	Value	Error
A_∞	123.01	0.10
A_0	127.95	0.08
k_{app}	0.0026	0.0001
R^2	0.9953	NA

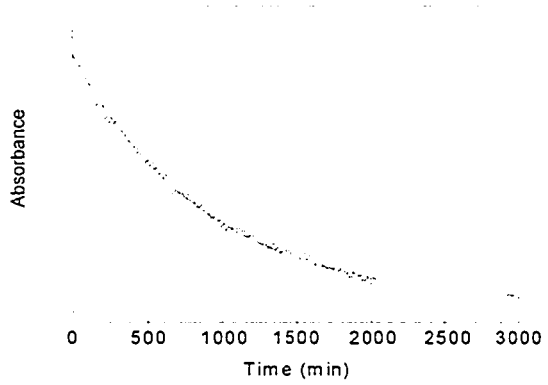

b

$A = A_\infty + (A_0 - A_\infty)\exp(-k_{app}t)$		
	Value	Error
A_∞	121.41	0.06
A_0	126.92	0.04
k_{app}	0.00113	0.00003
R^2	0.9957	NA

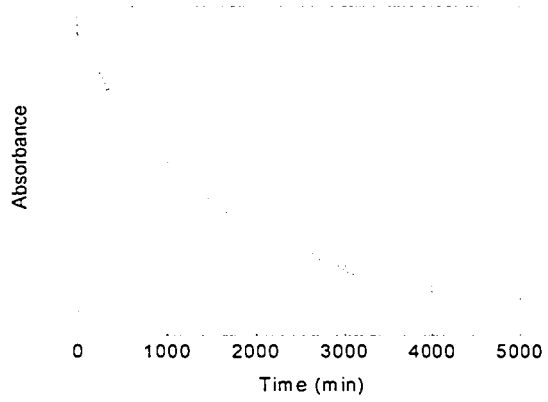

c

$A = A_\infty + (A_0 - A_\infty)\exp(-k_{app}t)$		
	Value	Error
A_∞	150.73	0.14
A_0	159.19	0.05
k_{app}	0.00062	0.00003
R^2	0.9992	NA

Figure 4.12 Time-resolved consumption of 80 Torr C_3H_6 during polymerization over $(\equiv SiO)_2Cr{=}CHC(CH_3)_3$, at (22.0±0.2)°C: (a) 1.60 wt.% Cr (m_{SiO2}=45 mg); (b) 1.23 wt.% Cr (m_{SiO2}=27 mg); (c) 0.79 wt.% Cr (m_{SiO2}=26 mg). Solid curves are three-parameter single exponential fits to the first-order integrated kinetic rate equation.

at similar temperatures (22.0 °C and 21.8 °C) with different Cr loadings and sample masses. The results are also shown in **Figure 4.12** and tabulated in **Table 4.1**. At (22.0±0.2)°C, k_{app} is proportional to the amount of Cr present regardless of Cr loading (0.79-1.60 wt.%), **Figure 4.13**. This suggests that the fraction of the active sites on silica surface is constant in this loading range. Furthermore, the intrinsic second-order rate constant for polymerization, k, is the slope of the plot of k_{app} as a function of the amount of Cr, equation 4.3.

$$-dP(C_3H_6)/dt = k_{app}\, P(C_3H_6); \quad k_{app} = k\, m_{cr} \tag{4.3}$$

At (22.0±0.2)°C, k = (2.9±0.1)s^{-1}(mol Cr)$^{-1}$. This translates to an activity of 1.0x10^4 g PP/(h molCr atm) (PP=polypropylene).

4.5 Discussion

4.5.1 Initiation of ethylene polymerization

In this chapter, the previously reported ability of $(\equiv SiO)_2Cr{=}CHC(CH_3)_3$ supported on Aerosil 200 to initiate ethylene polymerization at room temperature and low pressures was confirmed, as was the inability of $(\equiv SiO)_2Cr(CH_2C(CH_3)_3)_2$ on Aerosil 200 to do the same. In fact, when $P(C_2H_4) < 100$

Table 4.1 Pseudo first-order rate constants k_{app} for C_3H_6 polymerization initiated by $(\equiv SiO)_2Cr{=}CHC(CH_3)_3$ at (22.0±0.2)°C

wt.%Cr	m_{Cr} (mg)	k_{app} (min^{-1}) [a]
1.60	0.726	0.00258 ± 0.0001
1.23	0.327	0.00113 ± 0.00003
0.79	0.207	0.00062 ± 0.00003

[a] Errors are from non-linear least squares fit to a single exponential function.

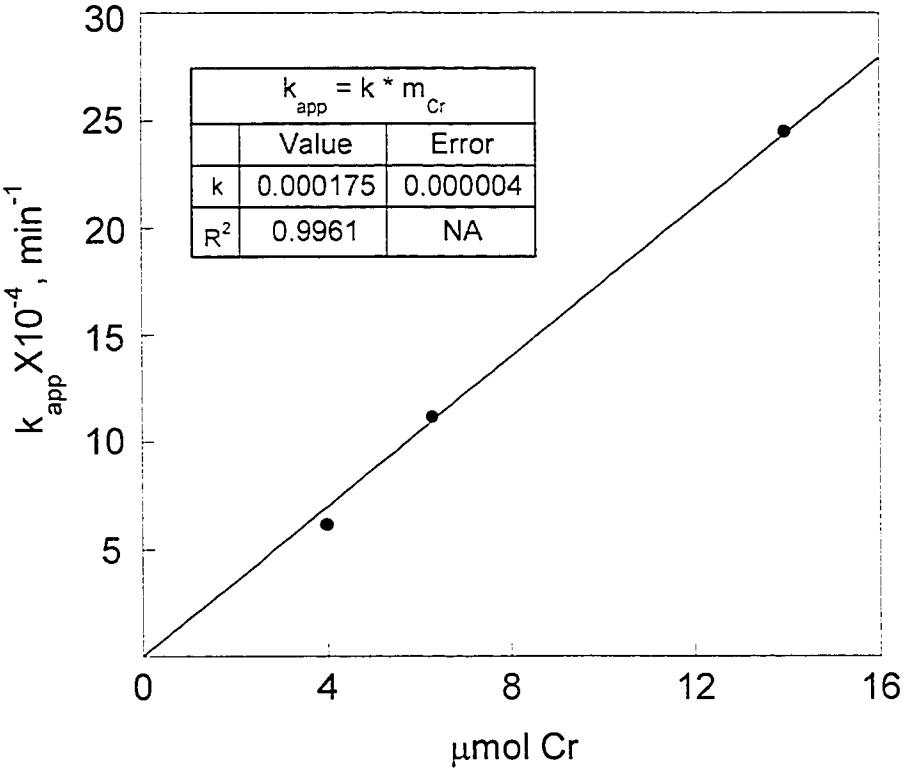

Figure 4.13 Dependence of the observed rate constant k_{app} for propylene polymerization initiated by $(\equiv SiO)_2Cr{=}CHC(CH_3)_3$ at (22.0±0.2)°C on the quantity of Cr.

Torr, a sample of $(\equiv SiO)_2Cr(CH_2C(CH_3)_3)_2$ showed polymerization activity only after heating to 70°C. During the prolonged induction period, thermal transformation of $(\equiv SiO)_2Cr(CH_2C(CH_3)_3)_2$ to $(\equiv SiO)_2Cr{=}CHC(CH_3)_3$ is presumed. The rate of the subsequent polymerization is much slower than the rate previously recorded with pre-formed $(\equiv SiO)_2Cr{=}CHC(CH_3)_3$ (section 4.2.1.2). Since the formation of $(\equiv SiO)_2Cr{=}CHC(CH_3)_3$ is much slower (section 3.2.3.2) than ethylene polymerization, the thermolysis reaction was not complete when ethylene polymerization was initiated. Consequently, the observed rate is determined by the slow thermolysis reaction.

The initiation of ethylene polymerization by $(\equiv SiO)_2Cr{=}CHC(CH_3)_3$ has been the subject of a computational study.[9] Schmid and Ziegler's model ethylidene complex **A** was shown to add ethylene to form the chromacyclobutane **B** with no barrier, **Scheme 4.1**. The [2+2] addition is exothermic by 38.9 kcal/mol, therefore **B** represents a strong thermodynamic sink for the alkylidene complex. From the chromacyclobutane **B**, two possible fates were investigated: (1) regeneration of an alkylidene site by a 1,3-hydrogen shift, to give **C**; or (2) insertion of a second equiv. of ethylene to give the chromacyclohexane **D**. For the former, the activation barrier was calculated to be a prohibitive 56.3 kcal/mol. This result means that the alkylidene is not a propagation intermediate in polymerization.

Ethylene insertion into the chromacyclobutane has a calculated barrier of 21.9 kcal/mol, and is exothermic by 32.5 kcal/mol. While this is a favorable process due to

Scheme 4.1 Model initiation sites according to Ziegler[9]

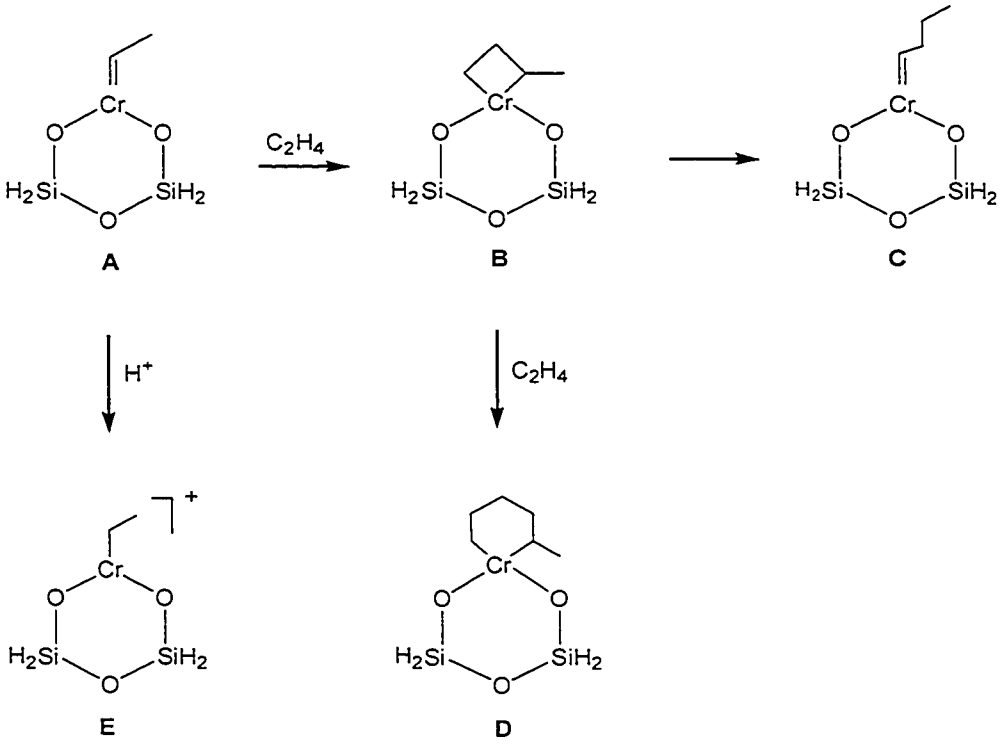

the relief of ring strain, the advantage is lost for subsequent ethylene insertions which form larger metallacycles. Although such a mechanism has been proposed for Cp_2Cr/Al_2O_3 polymerization catalysts,[16] the calculated barrier is inconsistent with experimentally measured values (ca. 8 kcal/mol).[5]

Similar conclusions were reached in a computational study by Espelid and Børve.[10] They considered three cluster models based on $H(OSiH_2)_nOH$ oligomers (n=1, 2, 3) as binding sites for chromium on the silica surface, **Scheme 4.2**. The ∠OCrO angle increases from 86° (for $n_{Si} = 1$) to 116° ($n_{Si} = 2$) and 135° ($n_{Si} = 3$). For $n_{Si} = 2$, the ∠OCrO angle is about 30° less than found for chromic acid $(HO)_2CrO_2$, indicating that the six-membered ring is strained. Nevertheless, this ring size was chosen to represent most of the silica-supported chromium sites, resulting in a model identical to that of Schmid and Ziegler.[9]

As in the previous study, Espelid and Børve calculated that [2+2] addition of ethylene to a chromium(IV) ethylidene has no activation barrier; furthermore, the energy of reaction is also similar, at -37.6 kcal/mol. Isomerization of the strained chromacyclobutane to a butylidene was investigated both as concerted 1,3-hydrogen transfer and via a Cr(VI) hydride intermediate. The former has a very high barrier, 57.3 kcal/mol. The latter is slightly more accessible, by ca. 7 kcal/mol, but is still too high to be considered plausible as a propagation step.

Scheme 4.2 Model initiation sites according to Børve[10]

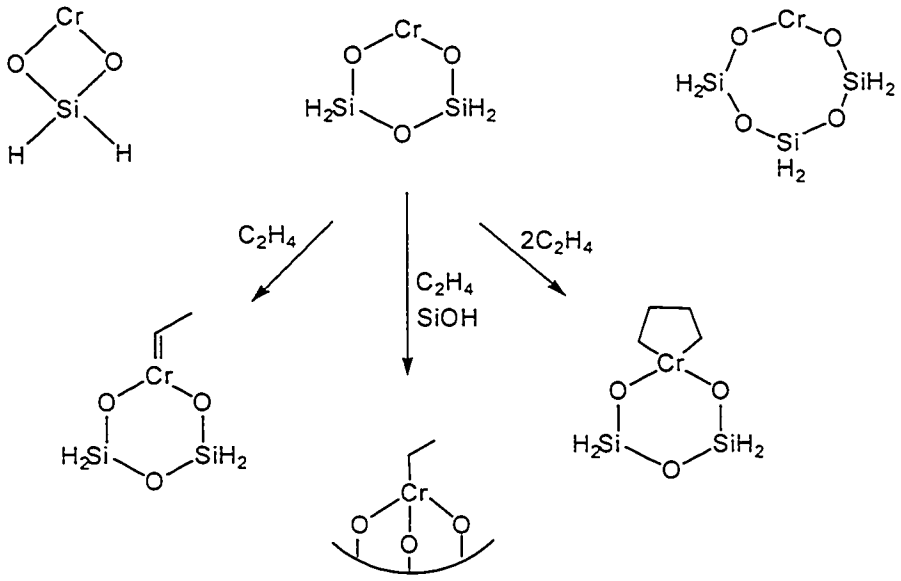

Direct insertion of ethylene into a chromacyclopentane was also investigated. The barrier was calculated to be 28.3 kcal/mol, with a reaction energy of -22.4 kcal/mol. These values are not much different from the corresponding values for direct insertion of ethylene into a dialkylchromium(IV) site, 27.0 and -23.7 kcal/mol, respectively. Although the barrier is lowered somewhat (to 19.6 kcal/mol) in the case of an (allyl)(alkyl)Cr(IV) reactant by η^3-allyl stabilization of the transition state, these values are still high enough to cause the authors to dismiss the possibility that either a metallacycle or a dialkyl species is the propagating site, regardless of the ∠OCrO angle of the anchoring site on silica (for angles between 90 and 180°).

In light of the findings of Ziegler and Børve, our observation that $(\equiv SiO)_2Cr(CH_2C(CH_3)_3)_2$ is capable of initiating ethylene polymerization at only slightly higher pressures (400 Torr ≤ P ≤ 1 atm) than $(\equiv SiO)_2Cr{=}CHC(CH_3)_3$ is truly surprising. Previously, the lack of activity of $(\equiv SiO)_2Cr(CH_2C(CH_3)_3)_2$ at low pressures (P < 400 Torr) was explained as arising form the steric bulk of the neopentyl ligands.[8] Now it seems that explanation may have to be reevaluated.

Schmid and Ziegler transformed their ethylidenechromium(IV) model into a cationic site by protonating the α-C with an acidic surface hydroxyl, **Scheme 4.1 E**. The cationic site binds ethylene and inserts with a very low barrier, 10.5 kcal/mol, suitable for a propagation site. Espelid and Børve discussed proton transfer to ethylene coordinated to Cr(II) to generate the same ethylchromium(IV) site.[17] However, they found that proton transfer from the silanol group is accompanied by a

strong covalent interaction between the siloxide oxygen and the chromium(IV) center, **Scheme 4.2**, precluding the formation of an isolated cation. The apparent activation energy for ethylene coordination and insertion at this pseudo-tetrahedral ethylchromium(IV) site is a plausible 6.3 kcal/mol, establishing this as a candidate for the propagating centre.

We infer that ethylene induces some transformation in our bis(neopentyl)chromium(IV) sites to activate them for polymerization, since direct ethylene insertion seems unlikely for all of the reasons described above. Unlike Ziegler and Børve, we are hesistant to invoke protonation by a neighboring silanol, since the silanol population as probed by *in situ* IR spectroscopy does not decrease upon addition of ethylene, **Figure 4.14**.

A more appealing explanation is that coordination of ethylene lowers the barrier to α-H elimination and thus causes $(\equiv SiO)_2Cr{=}CHC(CH_3)_3$ (or the chromacyclobutane) to be formed *in situ*. This explanation is bolstered by the detection of both neopentane and neohexene among the volatile products of polymerization initiated by $(\equiv SiO)_2Cr(CH_2C(CH_3)_3)_2$. Neopentane is presumed to arise by α-H abstraction induced by ethylene coordination. Neohexene is the characteristic product of olefin metathesis between ethylene and resulting $(\equiv SiO)_2Cr{=}CHC(CH_3)_3$. 4,4-dimethyl-1-pentene is another volatile product characteristic of the neopentylidene reaction with ethylene via cycloaddition followed by reductive elimination. We

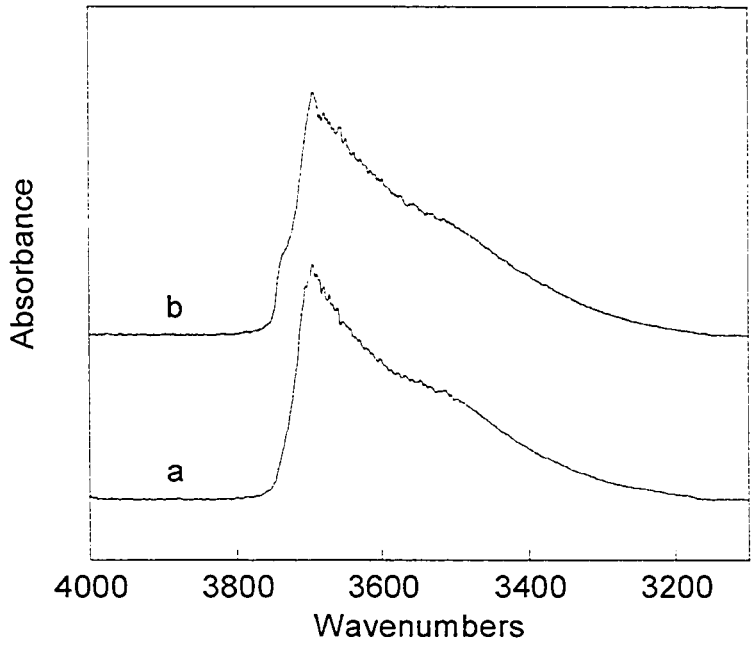

Figure 4.14 IR spectra of ν(OH) region (a) before; and (b) shortly after addition of 640 Torr C_2H_4 to $(\equiv SiO)_2Cr(CH_2C(CH_3)_3)_2$ on a 23.6 mg silica pellet of Aerosil 200 with 1.19 wt.% Cr.

note that all of these products may also arise via a chromacyclobutane intermediate formed directly from $(\equiv SiO)_2Cr(CH_2C(CH_3)_3)_2$ and ethylene, **Scheme 4.3**.

The question still remains, how does $(\equiv SiO)_2Cr{=}CHC(CH_3)_3$ initiate ethylene polymerization? According to the computational studies, the most favorable (barrierless) reaction of this site with ethylene is [2+2] cycloaddition to generate a chromacyclobutane. This intermediate is almost certainly the one to give rise to neohexene by [2+2] cycloreversion, in the process creating a methylidene site, $(\equiv SiO)_2Cr{=}CH_2$, which would then add C_2H_4 to give a new chromacyclobutane. β-H elimination from the chromacyclobutane has a very high barrier because the transition state is geometrically strained. We presume that the next step is direct ethylene insertion to generate a chromacyclohexane. Formation of an alkylchromium(IV) hydride from this site by β-H elimination is feasible, **Scheme 4.3**. Alternatively, ethylene may assist the ring-opening of the chromacyclobutane (β-H transfer to monomer), generating a dialkylchromium(IV) intermediate with a β-hydrogen. However, neither the metallacycle nor the alkylchromium(IV) hydride can be the propagating site for the reasons given above.

In order to account for the formation of a polymerization active site with a low ethylene insertion barrier, without invoking the participation of residual surface hydroxyls, we propose a new, two-site mechanism. Reductive elimination of silanol may occur from an alkylchromium(IV) hydride site, **Scheme 4.4**. Reaction of this silanol

Scheme 4.3 Proposed pathways to obtain volatile products over supported organochromium catalysts

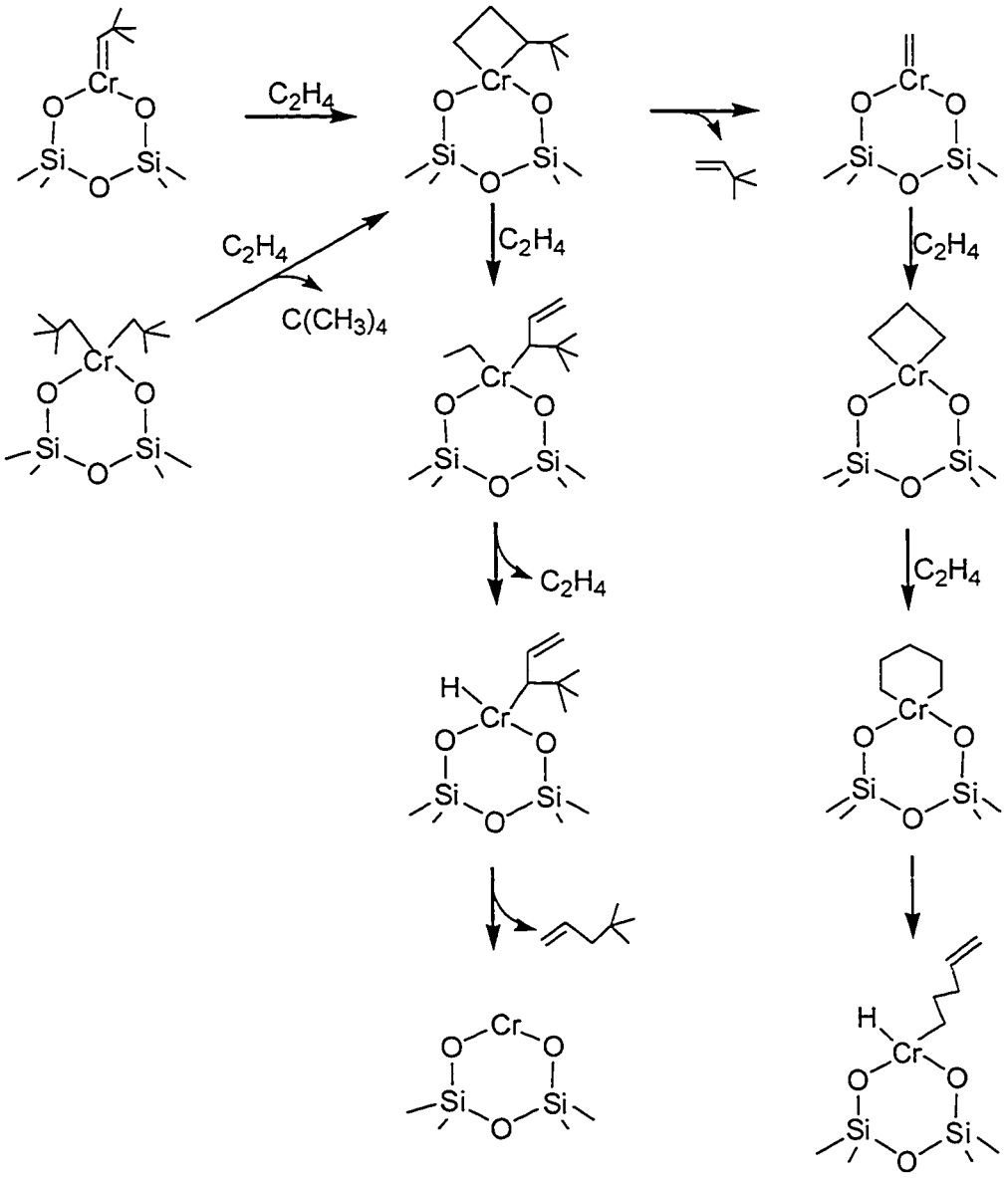

Scheme 4.4 Two site model for Cr/SiO_2 catalyst

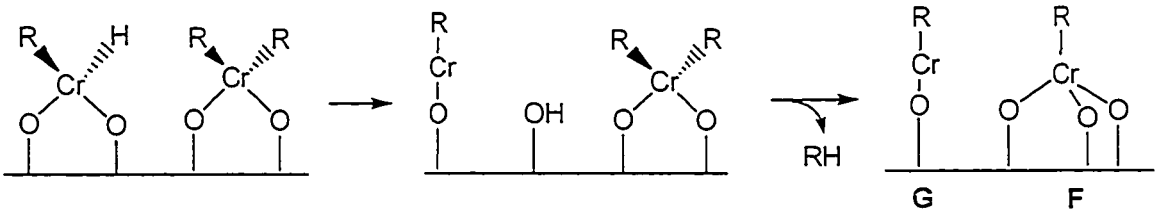

with an adjacent dialkylchromium(IV) site creates the propagation site **F** by elimination of alkane, without altering the residual silanol population. Interestingly, this proposal also generates an alkylchromium(II) site **G**. Phillips catalysts possess sites that generate ethylene oligomers in addition to sites which generate high molecular weight polymers.[18] Molecular chromium complexes which catalyze ethylene trimerization are also known, and Theopold has shown that organochromium(II) complexes tend to oligomerize rather than polymerize ethylene.[19,20] Cyclization of two equiv. of ethylene on the alkylchromium(II) site **G** to generate a chromocyclopentane, followed by ethylene insertion, would generate the chromacycloheptane intermediate proposed to be the source of 1-hexene (observed by us and in Phillips systems), **Scheme 4.5**.

Scheme 4.5 Proposed mechanism for 1-hexene formation

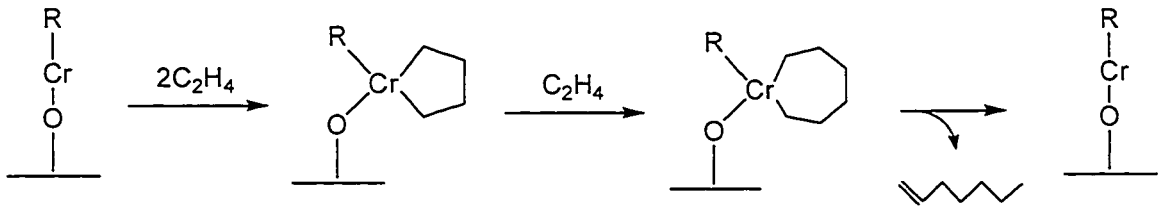

The difference in reaction channels of sites **F** and **G** is suggested to be a consequence of their abilities to bind one and two equiv. C_2H_4, respectively.

4.5.2 Inhibition of ethylene insertion by siloxane coordination

Another surprise in this research was the inability of Sylopol-supported $(\equiv SiO)_2Cr{=}CHC(CH_3)_3$ sites to react with low pressures of ethylene (< 400 Torr), since the stoichiometry of grafting and thermolysis was otherwise very similar to the Aerosil 200-supported chemistry. This divergence of Sylopol 952 and Aerosil 200 chemistry implies that the silica support plays an important role in the initiation of polymerization. It is possible that the siloxane stabilization of $(\equiv SiO)_2Cr{=}CHC(CH_3)_3$ described in the previous chapter is strong enough to prevent ethylene insertion. Since the strength of the siloxane-Cr interaction is dependent on the geometric structure of silica, which is expected to vary for different locations on the amorphous surface, it is reasonable to assume that ethylene can displace the siloxane ligand in some but not all of the supported complexes, equation 4.4.

$$(\equiv SiO)_2(\equiv Si_2O)Cr{=}CHC(CH_3)_3 + C_2H_4 \rightleftharpoons [(\equiv SiO)_2(C_2H_4)Cr{=}CHC(CH_3)_3] + \equiv SiOSi\equiv \quad (4.4)$$

According to this explanation, higher pressures of C_2H_4 should be able to activate more neopentylidene sites, due to the displacement of the equilibrium shown in equation 4.4. In agreement with this hypothesis, the threshold for inhibition of polymerization activity by O_2 increased from 20 to 30% poisoning of the Cr sites when the C_2H_4 pressure was raised from 60 to 250 Torr.[6] Further investigation of Sylopol 952 supported $(\equiv SiO)_2Cr{=}CHC(CH_3)_3$ showed that it does initiate polymerization in the presence of ca. 1 atm C_2H_4. We propose that spectroscopically undetected (thus far) siloxane coordination results in a stronger interaction with the potential active sites on the surface of Sylopol 952 than on Aerosil-200 surface, thereby inhibiting polymerization at lower pressures. This phenomenon is suggested to be a consequence of the surface roughness of the silica gel (with a surface fractal dimension close to 3.0),[21] resulting in greater proximity of adjacent siloxanes to the grafted Cr sites.

4.5.3 Rate of propylene homopolymerization

The rate of propylene polymerization was found to be slower than ethylene polymerization, as expected. Propagation rate constants for the various α-olefins investigated to date are compared in **Table 4.2**. In previous research, the rate constant for 1-hexene polymerization was measured to be 4.8 times slower than for ethylene

Table 4.2 Comparison of second-order rate constants for α-olefin polymerization initiated by $(\equiv SiO)_2Cr{=}CHC(CH_3)_3$ on A_{200}-200 at 21-22°C

Monomer	k $s^{-1}(mol\ Cr)^{-1}$	Reference
ethylene	177±3	previous work[22]
1-hexene	38±2	previous work[22]
propylene	2.9±0.1	this work

polymerization. Interestingly, propylene polymerization is even slower than 1-hexene polymerization.

The overall propagation rate is a consequence of two consecutive propagation steps. In the first, an ethylene π-complex is formed at the active site, equation 4.5. Coordination may be favored by back-donation of the Cr d electrons into the ethylene π* orbital, although not so much as to create a high barrier for the subsequent migratory insertion, equation 4.6.

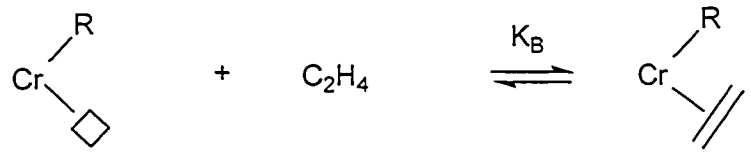

(4.5)

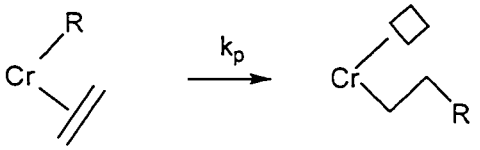

(4.6)

The observed rate constant is the product $K_B k_p$.

Clearly the overall rate of polymerization for a given α-olefin depends on both its ability to bind to the active site and the rate at which it undergoes insertion. These factors were evaluated independently in a study of olefin insertion into the metal-hydride bond of $Cp^*_2Nb(CH_2=CHR)H$.[23] Propylene insertion is 340 times faster than ethylene insertion at 50°C in this Nb(III) system (i.e., d^2, like Cr(IV)). This effect was explained by stabilization of the partial positive charge which develops at the β-carbon

in the insertion transition state. Therefore electron-donating substituents on the β-carbon lower the barrier for migratory insertion.

On the other hand, competitive binding experiments show that propylene coordination is less favorable than ethylene coordination. The value of K_{eq} for equation 4.7 is 0.0069.[23]

$$Cp^*_2Nb(C_2H_4)(H) + C_3H_6 \rightleftharpoons Cp^*_2Nb(C_3H_6)(H) + C_2H_4 \qquad (4.7)$$

In the case of our Cr/SiO_2 catalyst, the weaker binding of propylene compared to ethylene is the dominant effect, and is not compensated by faster migratory insertion of propylene. In this light, the faster reaction of 1-hexene relative to propylene is curious. Presumably the adsorption energy for gaseous 1-hexene on the surface is much greater than for propylene, while the rates of migratory insertion are more similar.

4.6 Conclusion

Ethylene polymerization at low pressures initiated by $(\equiv SiO)_2Cr{=}CHC(CH_3)_3$ on A_{200}-200 resulted in the same reactivity as previously reported. However, due to stronger interactions of siloxanes with active sites on the surface of Sylopol 952, higher pressures of ethylene were required for $(\equiv SiO)_2Cr{=}CHC(CH_3)_3$ to initiate polymerization on Sylopol silica. $(\equiv SiO)_2Cr(CH_2C(CH_3)_3)_2$ was shown to be capable of initiating

ethylene polymerization at high pressures on both Aerosil 200 and Sylopol 952. The *in situ* formation of $(\equiv SiO)_2Cr{=}CHC(CH_3)_3$ from $(\equiv SiO)_2Cr(CH_2C(CH_3)_3)_2$ was suggested by the identification of gas phase products during the polymerization. Pseudo-first-order propylene polymerization was observed to be a very slow process. Weaker binding of propylene compared to ethylene is considered to be the dominant factor controlling the slower rate of this reaction.

4.7 References

(1) Hogan, J. P. *J. Polym. Sci.: A-1* **1970**, *8*, 2637-2652.

(2) Clark, A. *Catal. Rev.* **1970,** *3,* 145-173.

(3) Wang, S.; Tait, P. J. T.; Marsden, C. E. *J. Mol. Catal.* **1991**, *65*, 237-252.

(4) Kaminsky, W.; Sinn, H. *Transition Metals and Organometallics as Catalysts for Olefin Polymerization;* Springer-Verlag: New York, 1988.

(5) Zakharov, V.; Yermakov, Yu. I.; *Catal. Rev.-Sci. Eng.* **1979**, *19*, 67-103.

(6) Scott, S. L.; Amor Nait Ajjou, J. *Chem. Eng. Sci.* **2001**, *56*, 4155-4168.

(7) Beaudoin, M. C.; Womiloju, O.; Fu, A.; Amor Nait Ajjou, J.; Rice, G. L.; Scott, S. L. *Inorg. Chim. Acta.* (in press).

(8) Amor Nait Ajjou, J. Ph.D. thesis, University of Ottwa, 2000.

(9) Schmid, R., Ziegler, T. *Can. J. Chem.* **2000**, *78*, 265-269.

(10) Espelid, Ø.; Børve, K. J. *J. Catal.* **2000**, *195,* 125-139.

(11) Ghiotti, G.; Garrone, E.; Zecchina, A. *J. Mol. Catal.* **1988**, *46*, 61-77.

(12) Bade, O. M.; Blom, R.; Dahl, I. M.; Karlsson, A. *J. Catal.* **1998**, *173*, 460-469.

(13) Painter, P. C.; Coleman, M. M.; Koenig, J. L. *The Theory of Vibrational Spectroscopy and its Application to Polymeric Materials*; Wiley: New York, 1982.

(14) Groeneveld, C.; Wittgen, P. P. M. M.; Swimmen, H. P. M.; Wernsen, A.; Schuit, G. C. A. *J. Catal.* **1983**, *83*, 346-361.

(15) Koenig, J. L. *Spectroscopy of Polymers;* Wiley: Washington, DC, 1992.

(16) Arean, C. O.; Platero, E. E.; Spoto, G.; Zecchina, A. *J. Mol. Catal.* **1989**, *56*, 211-219.

(17) Espelid, Ø.; Børve, K. J. *J. Catal.* **2002**, *205*, 366-374.

(18) Krauss, H. L.; Zums, E. *Z. Naturforsch* **1979**, *34B*, 1628.

(19) Emrich, R.; Heinemann, O.; Jolly, P. W; Krüger, C.; Verhovnik, G. P. J. *Organometallics* **1997**, *16*, 1511-1513.

(20) Theopold, K. H. *Eur. J. Inorg. Chem.* **1998**, 15-24.

(21) Avnir, D.; Farin, D.; Pfeifer, P. *New J. Chem.* **1992**, *16*, 439-449.

(22) Amor Nait Ajjou J.; Scott, S. L. *J. Am. Chem. Soc.* **2000**, *122*, 8968-8976.

(23) Doherty, N. M.; Bercaw, J. E. *J. Am. Chem. Soc.* **1985**, *107*, 2670-2682.

Chapter 5

General Conclusions

A. Confirmation of previous work: Grafting of $Cr(CH_2C(CH_3)_3)_4$, **1a**, and $Cr(CH_2Si(CH_3)_3)_4$, **1b**, by sublimation onto Aerosil 200 silica partially dehydroxylated at 200°C generates discrete mononuclear surface organometallic fragments, accompanied by the liberation of two equiv. of $C(CH_3)_4$ for **1a** and $Si(CH_3)_4$ for **1b**, as previously reported. $(\equiv SiO)_2Cr(CH_2C(CH_3)_3)_2$ was thermally transformed to a silica-supported neopentylidenechromium(IV) fragment by intramolecular α-H abstraction in a kinetically first order reaction. Metathetical exchange of $(\equiv SiO)_2Cr{=}CHC(CH_3)_3$ with styrene is also consistent with previous results. The ability of $(\equiv SiO)_2Cr{=}CHC(CH_3)_3$ on A_{200}-200 to initiate ethylene polymerization at room temperature and low pressures was also confirmed. The kinetics of polymerization are pseudo-first-order with a rate constant which is linearly dependent on the amount of Cr present.

B. Development of a new grafting technique: Deposition of $Cr(CH_2C(CH_3)_3)_4$ onto A_{200}-200 was achieved from solution. The resulting material appears to be identical in composition and reactivity to the material prepared by sublimation grafting. This finding greatly simplifies and accelerates catalyst preparation.

C. Influence of the silica support: Rather than being an inert component of supported chromium catalysts, the silica support has long been recognized as an essential participant in the coordination sphere of chromium, which consequently influences the olefin polymerization properties of supported chromium catalysts. Spectroscopic and stoichiometric (i.e., qualitative and quantitative) evidence leads us to conclude that the chemisorption of tetraneopentylchromium(IV) on partially dehydroxylated Sylopol 952 silica pretreated at 200°C results in the grafting of bis(neopentyl)chromium(IV) on two ≡SiOH groups, accompanied by the liberation of two equivalents of neopentane. This result is perfectly in accord with the grafting previously reported on Aerosil 200.

Identification of the volatile products of the subsequent thermolysis reaction by GC, infrared surface spectroscopy, and the reaction of alkylidene with styrene all confirmed that the bis(neopentyl)chromium fragment on Sylopol 952 undergoes thermolysis to generate a chromium neopentylidene, as on Aerosil 200. However, under the same reaction conditions as the Aerosil 200 supported neopentylidene, there is no obvious initiation of olefin polymerization by $(\equiv SiO)_2Cr{=}CHC(CH_3)_3$ on S_{952}-200 at ethylene pressures less than 400 Torr. We postulate that siloxane coordination results in a stronger interaction with the potential active sites on the surface of Sylopol 952 compared to Aerosil 200. Consequently, higher pressures of ethylene are essential to achieve the initiation of polymerization.

The ability of $(\equiv SiO)_2Cr(CH_2C(CH_3)_3)_2$ to initiate ethylene polymerization at high pressures of ethylene on both A_{200}-200 and S_{952}-200 was truly surprising. The

observation of neopentane, neohexene and 4,4-dimethyl-1-pentene among the volatile products of polymerization initiated by $(\equiv SiO)_2Cr(CH_2C(CH_3)_3)_2$ suggests the *in situ* formation of $(\equiv SiO)_2Cr{=}CHC(CH_3)_3$.

D. Rate of propylene polymerization: Kinetics of propylene polymerization were determined to be pseudo-first-order. The second-order rate constant for propylene polymerization was directly measured and found to be very small compared to other α-olefins. A combination of binding constant (thermodynamic) and insertion rate (kinetic) effects is proposed to account for the overall low rate.